
The Alien Space of Science: Sampling Coherent but Cognitively Unavailable Research Directions

Alejandro H. Artilés^{1,2,3}, Martin Weiss¹, Levin Brinkmann², Iyad Rahwan², Bernhard Schölkopf^{3,4}, Christopher Pal^{5,6,7}, Hugo Larochelle⁷, Anirudh Goyal, and Nasim Rahaman¹

¹Tiptree Systems

²Max Planck Institute for Human Development, Berlin

³Max Planck Institute for Intelligent Systems, Tübingen

⁴ELLIS Institute Tübingen

⁵Polytechnique Montreal

⁶Canada CIFAR AI Chair

⁷Mila – Quebec AI Institute

Abstract

Scientific discovery is constrained not only by what is true, but by what is cognitively available to the researchers currently exploring a field. Many directions are coherent in light of the literature yet unlikely to be proposed because no existing community occupies the right combination of concepts, methods, and intuitions. Modern language models inherit this bias, recombining high-density regions of the literature when prompted for novel ideas. We introduce a framework that targets the complementary region, which we call the **alien space of science**, where directions are plausible under the structure of existing knowledge but unlikely under the distribution of existing researchers. Our method first decomposes papers into granular conceptual units and clusters them into a shared vocabulary of *idea atoms*. It then learns two complementary models over this vocabulary. A *coherence model* scores whether a combination of atoms forms a viable research direction, and an *availability model* scores whether any existing author community is positioned to produce a given combination. Sampling alien directions then reduces to ranking atom combinations that maximize coherence while minimizing availability. On a corpus of 16,068 peer-reviewed LLM papers from NeurIPS, ICLR, ICML, and major NLP venues, the resulting sampler explores a 3.5–7× broader effective atom vocabulary than frontier LLM ideation baselines without sacrificing coherence, and produces ideas that match or exceed those baselines under blind LLM, human, and downstream experimental evaluation. By separating scientific plausibility from community availability, our framework points toward AI ideation that complements rather than merely accelerates human science, expanding exploration into coherent directions that the current community may overlook.

Code: <https://github.com/alejandrohdez00/alien-space-of-science>

1 Introduction

Scientific discovery is often described as a search through the space of possible ideas. But the space visible to a scientific community is only a small part of the space that may be scientifically coherent. Researchers inherit concepts, methods, collaborators, datasets, institutions, and disciplinary intuitions that make some directions easy to imagine and others effectively invisible. Two ideas may be equally plausible in light of the literature, yet differ dramatically in whether any existing researcher or community is likely to propose them.

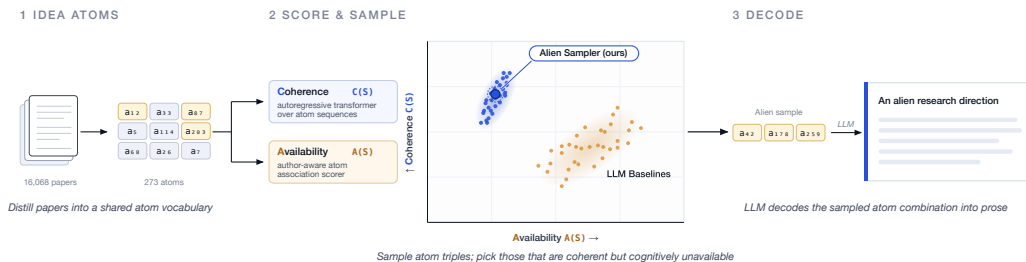


Figure 1: Overview of the Alien Science Sampling pipeline. Papers are distilled into conceptual units, which are clustered into a shared vocabulary of idea atoms. A coherence model learns which atom combinations form viable research directions, while an availability model estimates which combinations existing author communities are positioned to produce. Alien directions are sampled by maximizing coherence while minimizing availability.

We call the latter region the *alien space of science*: directions that are coherent under the structure of existing knowledge, but that do not naturally arise from the conceptual trajectories of existing researchers within a community. In hindsight such ideas may look obvious; before they appear, they sit outside prevailing taste and require expertise beyond what the field has already organized. They are not alien because they are speculative or unscientific; they are alien because they are cognitively unavailable to the community currently organized around the literature.

This distinction matters increasingly as large language models (LLMs) are used for scientific ideation. LLMs excel at synthesizing existing knowledge, but synthesis is not the same as escaping a field’s prior. When prompted for novel ideas, they tend to interpolate between fashionable concepts, salient mechanisms, and recurring research tropes already present in the literature. Rather than reliably helping researchers escape the community prior, they often approximate and amplify it [53, 37, 34, 38].

The central question of this paper is whether we can explicitly model and search beyond this prior. Rather than asking whether an idea is novel in an absolute sense, we ask whether it is *cognitively available* to the current scientific community [43, 39]. An idea is highly available if many researchers, given their past work, are naturally positioned to propose it; it is cognitively unavailable if it requires an unusual combination of concepts, methods, or intuitions not well represented by existing research trajectories.

This gives a two-axis view of scientific ideation. *Coherence* asks whether the components of an idea fit together in a way that could plausibly support a research contribution. *Availability* asks whether this combination is likely to be generated by the researchers and communities currently active in the field. Standard LLM ideation is often coherent but available. Random recombination can be unavailable but incoherent. The region we seek is the high-coherence, low-availability frontier: ideas that are simultaneously plausible and non-obvious.

To operationalize this view, we proceed in three steps. **First**, we decompose papers into short *conceptual units*¹ and cluster recurring units into a vocabulary of *idea atoms* (Section 3.1); each paper is represented as a sparse combination of such atoms. **Second**, we learn two complementary models over this discrete idea space: a *coherence model* (Section 3.2), trained on atom sets from papers, that scores whether a combination resembles a viable research direction; and an *availability model* (Section 3.3) that learns an author–idea compatibility function, scoring whether a community of existing researchers is positioned to produce it. **Third**, we sample combinations that maximize coherence while minimizing availability (Section 3.4); the high-coherence, low-availability frontier is what we call *alien science*.

Contributions. Our contributions are three-fold. **(a) Idea atoms.** We introduce a compositional representation of scientific directions, in which papers are mapped to sparse combinations over a shared, LLM-distilled vocabulary of recombinable idea atoms. **(b) Cognitive availability as a**

¹We provide an example of a conceptual unit here: “Polysemanticity in neural networks occurs when individual neurons respond to multiple, unrelated features (like ‘text’ and ‘dog faces’) due to superposition, which makes internal representations difficult for humans to interpret directly.”. Examples of *idea atoms* can be found in Appendix E.1

search objective. We operationalize *cognitive availability* [43, 39] as a learnable, community-level author–idea compatibility score, and pair it with a coherence model to search the alien-science frontier. **(c) Empirical evidence for search beyond the community prior.** On a curated corpus of 16,068 LLM papers from NeurIPS, ICLR, ICML, and major NLP venues, we validate that conceptual units preserve paper content, show via temporal held-out evaluation that the scoring models recover three-atom combinations of future papers far above chance, and find that Alien sampling explores a 3.5–7× broader effective atom vocabulary than frontier LLM baselines while matching or exceeding them under blind LLM, human, and downstream experimental evaluation.

2 Related Work

AI-assisted scientific discovery. Automated discovery has a long history in mathematics, chemistry, and scientific modeling [23, 7, 21, 22]. Recent LLM-based systems such as AI-Scientist [26] and AlphaEvolve [30] extend this agenda to broader scientific and engineering settings, using language models to propose, implement, evaluate, and refine candidate discoveries [33, 14]. Our focus is the ideation step inside this broader loop: how should a system choose which directions to investigate?

The ideation bottleneck. LLMs are increasingly competent at literature synthesis, coding, experimental design, and scientific writing [49, 25, 46]. Yet open-ended ideation exposes a distinctive failure mode: models repeatedly return to a narrow region of familiar concepts, templates, and methodological motifs [37, 11, 18], also flagged by Lu et al. [26]. We interpret this as a community-prior problem. The issue is not merely low novelty; the issue is that plausibility is often achieved by staying close to the distribution of existing researchers.

Retrieval- and feedback-augmented ideation. Systems such as SCIMON [45], ResearchAgent [5], and AI Co-Scientist [12] augment LLMs with literature retrieval, knowledge graphs, review loops, and refinement procedures. These systems improve grounding and execution, but they often begin from a human-supplied seed concept, core paper, or problem formulation. Since human seeds tend to come from cognitively available regions, the downstream system can inherit the same bias.

Concept recombination. A closer line treats the LLM as a decoder over externally supplied concept combinations: the system constructs a non-trivial combination from the literature and asks the model to reason over it [54, 41, 32]. We share the view that novelty can be induced by placing the model in a conceptual state it would not naturally reach. We differ in two ways. First, prior systems often operate over coarse keyword-level concepts such as *LLM*, *RAG*, or *MCTS*; we construct a content-bearing vocabulary bottom-up from paper-level methodological statements. Second, prior systems sample by random choice, human choice, or distance heuristics; we learn a search objective that explicitly separates coherence from availability.

Compositional skill representations. Our representation is also related to recent work that treats language-model behavior as composition over reusable skills. Arora and Goyal [2] give a theoretical account in which complex capabilities arise from combinations of elementary skills. Building on this perspective, Skill-Mix [50] evaluates whether models can flexibly combine randomly selected subsets of skills, while metacognitive skill-labeling work [10] shows that LLMs can elicit and cluster interpretable skill labels for problem solving. Instruct-SkillMix [20] uses this idea constructively: it extracts instruction-following skills with an LLM and generates synthetic data from random skill pairs to improve instruction tuning. Our idea atoms play an analogous compositional role, but differ in both source and objective. They are not task skills or instruction-following labels; they are methodological units distilled bottom-up from scientific papers. Moreover, rather than relying on random skill mixtures, we learn a coherence model and an author-conditioned availability model, allowing us to search for combinations that are simultaneously scientifically plausible and cognitively unavailable to the current research community.

Cognitive availability and scientific surprise. Surprising combinations of research content can predict outsized scientific impact, especially when they bridge distant intellectual regions [36]. Other work operationalizes surprise, novelty, or unexpectedness for active discovery [1, 19, 37, 34, 3, 53]. We target a related but distinct construct: *cognitive availability* [43]. Sourati and Evans [39] model collective scientific attention through random walks on a researcher–concept hypergraph. We adapt the availability intuition to a generative setting, replacing graph distance with a learned

dual-encoder model that scores whether author communities are positioned to produce a full research direction. While walk-based distances can capture meaningful structure in domains with narrow author specialization and enumerable vocabularies, ML researchers publish broadly across subareas, making nearly every atom pair reachable within two hops. As a result, direct hypergraph approaches largely collapse in this setting (Appendix A.9).

3 Method

The method follows directly from the thesis. To search coherent directions outside the community prior, we need: a representation of research directions, a model of scientific coherence, a model of community availability, and a search objective that trades them off.

3.1 Representing Research Directions as Idea Atoms

Corpus. We collect 16,068 papers on large language models from major machine learning and NLP venues, including NeurIPS, ICLR, ICML, and major NLP conferences. The domain is typically dense and methodologically diverse, yet bounded enough to approximate broad coverage. This matters for availability modeling: when a direction is estimated as unavailable, the estimate should reflect a real absence from the author community rather than missing data. Extending to the broader ML or AI literature is left to future work; it would require substantially greater data coverage, compute, and budget.

Conceptual units. Raw papers are too entangled for recombination. They include citations, repeated motivation, formatting, experimental detail, and result-specific context. We therefore first compress each paper into a methodological summary focused on mechanisms, objectives, architectures, training procedures, evaluation setups, and technical insights. We then prompt an LLM to extract *conceptual units*: short, self-contained statements describing a technique, mechanism, objective, architectural choice, or evaluation procedure. Each unit states both what is done and why it matters, and must be understandable without the original paper. This focus on methodology is deliberate: methods contain the recombinable conceptual building blocks we wish to sample over, whereas experimental results are environment-dependent outcomes that cannot be meaningfully recombined.

Idea atoms. Many conceptual units express the same reusable idea in different language. We embed all units and cluster them with HDBSCAN [8, 28]; each cluster is summarized into a canonical description using an LLM. The result is an *idea atom*: a recurring conceptual building block shared across papers. The final representation gives a vocabulary of 273 atoms and a sparse mapping from each paper to the atoms it expresses. Appendix E.1 gives examples.

This representation is designed to sit between keywords and full papers. Keywords are too coarse to encode mechanism; full text is too specific to recombine. Idea atoms are small enough to compose, but rich enough to preserve methodological content.

3.2 Modeling Scientific Coherence

Coherence asks whether a set of atoms may plausibly co-occur in one paper. We model coherence with an autoregressive Transformer [44], treating each atom as a discrete token. At train time, each paper’s atoms are presented as multiple random serializations, so the model captures paper-level co-occurrence structure without committing to a canonical ordering.² For an atom set $S = \{a_1, \dots, a_n\}$ serialized as (a_1, \dots, a_n) , the model optimizes next-atom prediction $p_\theta(a_t | a_{<t})$. We score coherence by length-normalized log likelihood:

$$C(S) = \frac{1}{|S|} \sum_{t=1}^{|S|} \log p_\theta(a_t | a_{<t}).$$

High $C(S)$ indicates that the atoms in S plausibly co-occur within a single paper. We use this model both to generate candidate atom sets and to score arbitrary combinations.

²In practice, we show that at inference time, the model is robust to order variance, being able to distinguish between real papers, random combinations and disjoint examples regardless of ordering (see Appendix 8).

3.3 Modeling Cognitive Availability

Availability is relational: an idea is available *to someone*. We model this by learning an author–idea compatibility function. For each author i , let R_i be the author’s repertoire: the union of atoms across all their papers. We randomly split R_i into a query subset Q_i and a complement $R_i \setminus Q_i$. These are two disjoint views of the same research trajectory.

We train two encoders, ϕ and ψ , that share an atom embedding table. The set encoder ϕ embeds the query subset with a bidirectional Transformer without positional encodings, mean-pools the output, projects it, and L2-normalizes it. The author encoder ψ embeds the complement as a larger bag of atoms, mean-pools, applies an MLP, and L2-normalizes. This asymmetry reflects the problem: a candidate idea is a small structured combination, while an author repertoire is a broader distribution over interests.

For a batch of B triples $(i, Q_i, R_i \setminus Q_i)$, we form scaled cosine logits

$$\ell_{ij} = \tau \psi(R_i \setminus Q_i)^\top \phi(Q_j),$$

with learned temperature τ , and minimize the symmetric InfoNCE loss

$$\mathcal{L} = \frac{1}{2B} \sum_{i=1}^B [\text{CE}(\ell_{i,:}, i) + \text{CE}(\ell_{:,i}, i)].$$

Rows ask each author representation to identify its held-out query; columns ask each query to identify its author. We mask off-diagonal entries that share an author, since different subsets from the same author are unlabeled positives rather than true negatives.

The disjoint split is crucial. If the author encoder could see Q_i , the model could solve the task through raw atom overlap. Holding Q_i out forces the model to learn which atoms tend to belong together within a researcher’s trajectory, placing author i near the kinds of atom subsets they are likely to produce.

At inference, we precompute $\psi(R_i)$ for all authors using their full repertoires. For a candidate atom set S , we compute $\phi(S)$ and score it against every author by cosine similarity. We aggregate the top- m author similarities by their median:

$$A(S) = \text{median}_{i \in \text{Top}_m(S)} \psi(R_i)^\top \phi(S).$$

High $A(S)$ means that a community of authors is close to the research direction. A low $A(S)$ indicates that no known m -author community is strongly aligned with the combination. We define unavailability as $U(S) = -A(S)$.

Taking the median over the top- m rather than the top-1 is what enforces this community reading: in AI/ML, a few authors publish across many subfields and can cover atom combinations that no coherent group actually supports, so requiring the next-best authors to also match prevents a single generalist from single-handedly marking an idea as available.

3.4 Sampling the Alien Space

Given coherence $C(S)$ and unavailability $U(S)$, sampling alien directions becomes ranking candidate atom sets. For a candidate pool, we compute within-pool z -scores $z_C(S)$ and $z_U(S)$, then rank candidates by

$$F_\beta(S) = (1 - \beta)z_C(S) + \beta z_U(S), \quad \beta \in [0, 1].$$

The parameter β controls how aggressively the sampler moves away from the community prior. At $\beta = 0$, the sampler selects the most paper-like combinations. At $\beta = 1$, it selects the least available combinations, often sacrificing plausibility. The intended regime is intermediate: far enough from existing author communities to be cognitively unavailable, but coherent enough to support investigation.

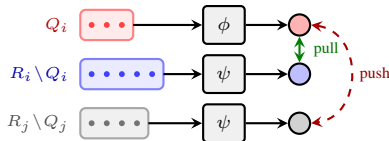


Figure 2: Two-encoder contrastive training for cognitive availability. A held-out query subset Q_i is encoded by ϕ ; the complement $R_i \setminus Q_i$ and other authors’ complements are encoded by ψ . Disjoint views of the same author are pulled together, while views from different authors are pushed apart.

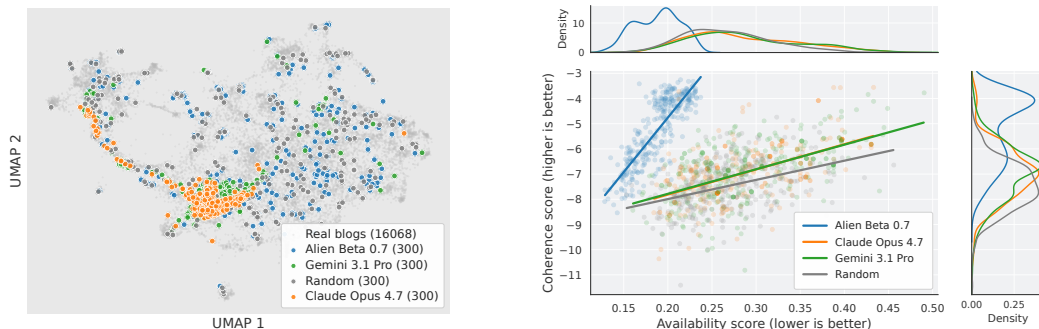


Figure 3: Generated ideas in embedding and score space. **Left:** UMAP embedding of method digests from the 16,068-paper corpus and decoded ideas from Claude, Gemini, Alien, and Random samples. Claude and Gemini concentrate around sparse-autoencoder and interpretability concepts, while Alien samples occupy a broader region. **Right:** Coherence–availability scores for generated three-atom combinations. Higher coherence and lower availability are preferred. Alien sampling at $\beta = 0.7$ concentrates in the intended high-coherence, low-availability region, while LLM baselines stay closer to more available regions and random sampling loses coherence.

A selected atom set is not yet a readable proposal. We therefore pass the atoms and their canonical descriptions to a fixed decoder LLM, prompted to synthesize a short research-idea sketch that uses every atom (see Appendix E.2 for idea examples). The same decoder is used for all methods in downstream comparisons, so differences reflect which atoms were selected rather than which model wrote the final prose. We fix $\beta = 0.7$ for the main experiments, selected by an originality–coherence sweep reported in Appendix A.11.1. Decoder details and stability diagnostics are reported in Appendix B.

4 Experiments

We evaluate the framework in five stages. First, we test whether idea atoms preserve paper-level methodological content. Second, we validate that coherence and availability are learnable, distinct axes. Third, we ask whether these axes recover future research directions in a temporal held-out setting. Fourth, we test whether Alien sampling changes the distribution of ideation without sacrificing quality. Finally, we evaluate whether the generated ideas remain competitive under expert human review and downstream autoresearch execution.

4.1 Idea Atoms Preserve Paper-Level Methodological Content

A useful atom space must compress papers into reusable components without collapsing distinct mechanisms into vague clusters. We therefore validate the representation layer in two stages: extraction fidelity before clustering, and semantic separability after clustering.

Conceptual-unit fidelity. Before clustering, we test whether extracted conceptual units preserve the methodological content of their source papers. For each paper, we reconstruct its methodological summary using only its conceptual units and ask an LLM judge to compare the reconstruction against the original summary. The judge evaluates mechanism equivalence rather than surface overlap: exact names, constants, and dataset details are not required, but the reconstructed text should describe the same method. Conceptual-unit reconstructions receive full-match judgments for 97% of evaluated papers. This validates the extraction step: the pipeline begins from content-bearing methodological statements rather than isolated keywords.

Atom purity and coverage. Clustering turns paper-specific units into reusable atoms. We evaluate candidate clusterings with two LLM-judged semantic tests over the original unit text. In an *intruder* task, the judge sees four units from one cluster and one unit from a neighboring cluster and must identify the odd one out. In an *overlap* task, the judge sees units from two nearby clusters and must partition them into two coherent groups; we score the partition with adjusted Rand index. The best configuration embeds 82,255 conceptual units with BAAI/bge-large-en-v1.5 [48], reduces them with UMAP, and clusters with HDBSCAN, obtaining 273 well-defined clusters according to our

metrics. Then, we use an 80% coverage operating point, increasing the average from 1.65 to 3.38 atoms per paper, covering 99.5% of papers with at least one atom and 90.6% with at least two. This point preserves semantic separability while producing enough co-occurrence signal for downstream models. Full method and hyperparameter sweeps are reported in Appendix B, Figures 20 and 21. Reassignment/coverage diagnostics can be found in Appendix B and Figure 22.

4.2 Coherence and Availability Are Learnable, Distinct Axes

Before using the scores for generation, we test whether they behave as intended on controlled atom-set pools. For coherence, we compare exact paper atom sets, uniformly random atom sets, and pairwise-disjoint atom sets whose atom pairs never co-occur in the training corpus. The coherence model ranks paper matches highest, random sets lower, and disjoint sets lowest for both $k = 3$ and $k = 4$ atom sets, being k the number of atoms in the combination. For availability, we compare high-author-support sets, random sets, and zero-support sets absent from every author repertoire. The availability model ranks high-support sets above both controls, again for both $k = 3$ and $k = 4$. These diagnostics establish that the two scores are interpretable and distinct: coherence captures paper-like compatibility, while availability captures alignment with author communities (see Figure 23).

4.3 The Scores Recover Future Research Directions

A stronger test is whether the learned scores recover combinations that become real papers after the training cutoff. Our corpus spans 2017–2025, with 2025 contributing 7,920 of 16,068 papers. We train both scoring models only on papers through 2024 and rank all possible three-atom combinations, then compare the top-ranked triples against the 2,477 unique three-atom sets observed in held-out 2025 papers.

For $k = 3$, exhaustive evaluation is feasible: we rank all triples and compare the top 1000 against the 2,477 unique three-atom sets observed in 2025 papers. A uniformly random top-1000 contains only 0.739 held-out sets in expectation. As shown in Figure 4, the coherence-only ranking ($\beta = 0$) recovers 23 held-out 2025 atom sets, a $31.1\times$ enrichment over this matched random baseline; the result is stable across retrieval cutoffs from $K = 100$ to $K = 10,000$ (Appendix 19).

Adding the availability term changes which future directions are recovered. As β increases, exact recall falls, but surviving hits move toward less crowded regions that nevertheless materialize as real papers. At $\beta = 0.7$, the triple corresponding to *Cosmos: Compressed and Smooth Latent Space for Text Diffusion Modeling* [29] appears at rank 19; a uniformly random top-100 would contain only 0.074 held-out 2025 triples in expectation. *Cosmos* was a NeurIPS 2025 paper whose open meta-review cited “**solid technical contributions to an underexplored area**” [31] as the primary reason for acceptance, exactly the kind of region the alien objective is meant to surface.

Method	Top-10 ↓	Eff. cov. ↑
Alien (Ours)	34.3%	72.5%
Gemini	76.7%	20.6%
Claude	95.7%	10.5%

Table 1: Diversity of generated atom combinations. Alien spreads probability mass across the atom vocabulary, while LLM baselines concentrate on a small subset.

As they may require a longer evaluation horizon, an effect also observed in Sourati and Evans

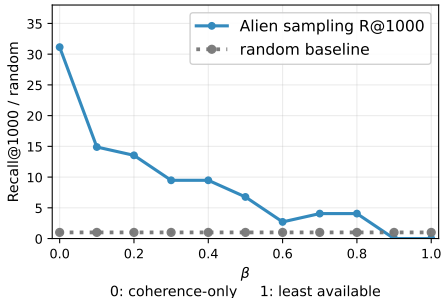


Figure 4: Temporal validation against held-out 2025 papers. Models are trained only through 2024. All $\binom{273}{3}$ triples are ranked and evaluated by exact recovery of 2025 three-atom paper sets in the top 1000.

A complementary paper-level ranking over 1,712 scorable NeurIPS 2025 papers places *Cosmos*, *Crucible* [17] (LLM agents for control-algorithm tuning), and *Meta CLIP 2* [9] (worldwide multilingual CLIP, NeurIPS 2025 spotlight) as the top three at $\beta \in [0.7, 0.8]$ (Appendix 12). The aggregate result matters more than any single example: the scores recover future research structure, and the availability term shifts the frontier toward less crowded directions.

Consistent with Sourati and Evans [39], our model predicts more available directions than unavailable ones. Estimates of unavailable directions are likely conservative, as they may require a longer evaluation horizon, an effect also observed in Sourati and Evans

[39]. Given that 2024–2025 account for most LLM-related research in our corpus, we focus on one-year-ahead predictions.

4.4 Alien Sampling Changes the Ideation Distribution Without Sacrificing Quality

We now evaluate the sampler as an ideation method. We fix the number of atoms per idea to 3, close to the corpus mean of 3.38 atoms per paper. We compare Alien against Claude Opus 4.7 and Gemini 3.1 Pro, each queried 300 times with the full atom vocabulary in context and prompted to select novel yet feasible combinations. Atom order is shuffled per query to mitigate positional bias. We also include 300 uniformly random atom triples. Alien selects 300 triples by ranking all candidate combinations with F_β at $\beta = 0.7$.

Score-space behavior. Figure 3 shows that Alien samples concentrate in the high-coherence, low-availability region. LLM baselines remain more available, while random combinations lose coherence and are surprisingly not as unavailable as desired. In a dense research domain, many random triples are still close to some author community; reaching the low-availability tail requires explicit search (see Appendix A.10).

Effective vocabulary coverage. We measure atom-space diversity using effective atom coverage, $\exp(H(p))/|\mathcal{A}|$, where $p(a)$ is the empirical frequency of atom a across generated combinations. We also report top-10 concentration: the fraction of generated combinations containing one of a method’s ten most-used atoms.

Table 1 shows the key distributional result. Alien’s ten most-used atoms appear in 34.3% of combinations, compared with 76.7% for Gemini and 95.7% for Claude. Alien’s effective atom coverage is 72.5%, compared with 20.6% and 10.5%. Random sampling remains the diversity ceiling, covering 97.4% of atoms with 86.6% effective coverage, but it does not optimize coherence or unavailability. Alien retains much of random sampling’s breadth while preserving scientific structure. This is the core failure mode of direct LLM ideation: the ideas are often fluent and plausible, but the underlying vocabulary collapses.

Blind pairwise judging. Diversity would not matter if the ideas were incoherent or uninteresting. We evaluate decoded ideas with blind forced-choice comparisons. A GPT-5.5 judge chooses which idea better occupies the coherent-but-cognitively-unavailable region: plausible enough to investigate, but more likely to expose a new framing or future research vein than to instantiate a familiar recipe.

On a balanced 50-idea-per-method tournament, Alien wins 55.6% of its matches, comparable to Gemini (54.4%) and above Claude (48.9%) and Random (41.1%). The more important result is in the tail. After selecting the top half and then the top ten ideas within each method from the previous round, Alien’s win rate rises from 55.6% on the full pool to 72.2% in the top-half pool and 69.4% in the top-ten pool. Claude falls from 48.9% to 27.8% and 30.6%; Gemini remains around 58–59%; Random remains around 41%. Alien is therefore not merely broader. It produces a stronger high-upside tail of cognitively less available but still plausible research directions.

4.5 The Effect Survives Contact with Reality: Human and Downstream Experimental Evaluation

We run two downstream tests. First, third-party expert human raters evaluate decoded idea descriptions directly. Second, a fixed autoresearch pipeline iteratively refines each idea, runs bounded experiments, and produces a research report; those reports are evaluated by blind pairwise judging.

Human evaluation. We collect 40 blinded reviews from 10 humans with post-graduate degrees in machine learning or computer science. Reviewers rate one idea at a time on coherence, feasibility, novelty, promise, obviousness, and overall quality. Alien and Claude tie on overall quality (4.03), followed by Random (3.75) and Gemini (3.68). Alien has the highest mean feasibility (3.90) and novelty (3.90), while Claude has the highest promise score (4.40). Thus human readers judge Alien ideas as competitive with the strongest LLM baseline, despite Alien occupying a substantially broader atom-space region.

Autoresearch execution. We run 40 generated ideas, 10 from each source, through a fixed autoresearch pipeline. The pipeline iteratively refines each idea, runs bounded experiments on A100 40GB

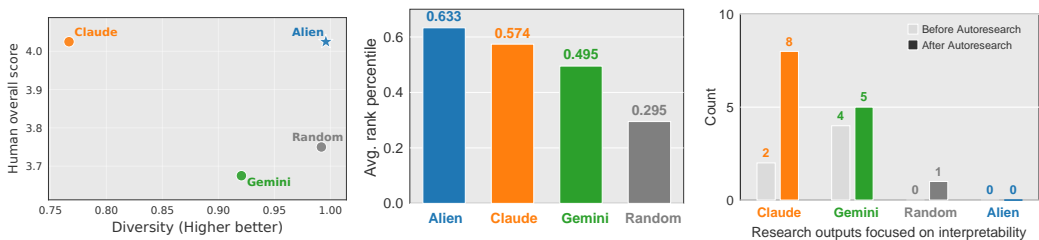


Figure 5: Downstream evaluations of generated ideas. **Left:** Human raters score Alien and Claude equally on overall quality, while Alien occupies a much higher-diversity region (diversity is computed based on the atoms present in the 10 ideas produced by each method). **Middle:** After autoresearch execution and blind Swiss-style pairwise judging, Alien has the highest average rank percentile and contributes 3 of the top 5 reports. **Right:** Autoresearch exposes a collapse mode: during the autoresearch loop, Claude and Gemini outputs concentrate toward interpretability-related themes, while Alien outputs do not.

GPU nodes, and produces a standalone research report. A blind LLM judge evaluates the reports using a six-round Swiss-style pairwise schedule with both A/B and B/A orderings, yielding 224 forced-choice comparisons. Converting preferences to ranks, Alien achieves the best average rank percentile over the pool (0.633), followed by Claude (0.574), Gemini (0.495), and Random (0.295). Alien also contributes 3 of the top 5 reports and 4 of the top 10 reports.

Motif collapse in LLM baselines. The same report set reveals a qualitative failure mode in the LLM baselines. Claude and Gemini outputs increasingly collapse toward interpretability: Claude shifts from 2/10 to 8/10 reports focused on interpretability, while Gemini shifts from 4/10 to 5/10. In contrast, Random changes from 0/10 to 1/10, and Alien remains at 0/10 before and after the autoresearch pipeline. Crucially, this collapse occurs *during* the autoresearch loop rather than at initial generation: even ideas not explicitly framed around interpretability are sufficiently close in concept space that iterative refinement pulls them toward this familiar attractor. Alien-generated ideas, which by construction occupy lower-availability regions, do not exhibit this collapse.

Summary. The evidence supports the full chain. Idea atoms preserve paper-level content. Coherence and availability behave as distinct learnable axes. The scores recover future paper combinations far above chance. Most importantly, Alien sampling changes the ideation distribution while preserving quality: it expands effective search beyond LLM baselines and avoids the motif collapse revealed by downstream execution.

5 Discussion

This paper argues that AI-assisted science should distinguish two quantities that are often conflated: whether an idea is scientifically plausible, and whether the current scientific community is likely to think of it. Modern LLMs are strong at the first kind of modeling. They can synthesize papers, produce coherent proposals, and extend familiar research programs. But because they are trained on the literature and prompted through language, they also inherit the distributional shape of that literature. They tend to search where the community has already placed conceptual mass. The result is a form of ideation that can be useful and fluent, but not necessarily complementary.

The alien space of science names the complementary target: directions that are coherent under existing knowledge but cognitively unavailable under the current community prior. This is not a claim that alien ideas are guaranteed breakthroughs. Most research ideas, even good ones, will fail. The claim is instead distributional: if AI systems are to expand science rather than merely accelerate it, they should move some coherent search mass into regions the community is unlikely to explore on its own.

Alien Sampling is one operationalization of this principle. The method is simple once the distinction is made. Represent research directions compositionally; learn which combinations are coherent; learn which combinations are available to existing authors; and search for high coherence with

low availability. The empirical results support this decomposition. Idea atoms preserve paper-level methodological content. Coherence and availability behave as distinct learnable axes. The learned scores recover future paper combinations far above chance. Most importantly, the sampler changes the distribution of generated ideas: it explores a much broader effective atom vocabulary than frontier LLM baselines while remaining competitive under human and downstream execution-based evaluation.

The broader implication is that AI-science systems should be evaluated not only by novelty, quality, or downstream task performance, but by *availability-adjusted discovery value*: how much coherent scientific search mass they move outside the current community prior. An AI scientist that produces more high-quality versions of already-available ideas may improve throughput. An AI scientist that reliably surfaces coherent, low-availability directions can change what the field explores. This axis is especially important as automated research systems become more capable: without an explicit pressure away from the community prior, more powerful systems may simply industrialize the production of familiar ideas.

This perspective also reframes the role of language models in scientific creativity. In our framework, the LLM is not asked to be creative from scratch. It distills papers, extracts conceptual units, summarizes atoms, and decodes selected combinations into readable proposals. The exploratory pressure comes from explicitly modeling the community prior and searching against it. This division of labor suggests a general design pattern for AI-assisted discovery: use language models as semantic interfaces, but use explicit search objectives to decide where in idea space they should operate.

Limitations. The current system can only recombine concepts already present in the literature. Truly new primitives require online vocabulary expansion, interaction with experiments, or mechanisms for creating atoms that are not already latent in the corpus. Availability is inferred from publications, which omit private reading, tacit knowledge, unpublished projects, failed attempts, and latent expertise. Human and LLM evaluations of open-ended ideas are noisy, and downstream autoresearch pipelines are imperfect proxies for real scientific programs. Finally, the strongest validation would be longitudinal: whether ideas estimated as coherent but unavailable later become productive research directions. Such evidence takes years, and the one-year temporal validation in this paper should be viewed as an early proxy rather than a final test.

Outlook. The broader agenda is to make the structure of scientific attention explicit. A field’s literature contains not only what has been discovered, but also a map of what its researchers are likely to notice next. Modeling that map enables a different kind of AI scientist: one that does not merely follow the community prior, but searches its coherent blind spots. If scientific progress depends partly on escaping what is currently easy to imagine, then the next generation of AI ideation systems should be judged by their ability to expand the visible space of science itself.

References

- [1] Dhruv Agarwal, Bodhisattwa Prasad Majumder, Reece Adamson, Megha Chakravorty, Satvika Reddy Gavireddy, Aditya Parashar, Harshit Surana, Bhavana Dalvi Mishra, Andrew McCallum, Ashish Sabharwal, et al. Autodiscovery: Open-ended scientific discovery via bayesian surprise. In *The Thirty-ninth Annual Conference on Neural Information Processing Systems*, 2025.
- [2] Sanjeev Arora and Anirudh Goyal. A theory for emergence of complex skills in language models, 2023.
- [3] Alejandro H Artiles, Hiromu Yakura, Levin Brinkmann, Mar Canet Sola, Hassan Abu Al-haija, Ignacio Serna, Nasim Rahaman, Bernhard Schölkopf, and Iyad Rahwan. Cultural alien sampler: Open-ended art generation balancing originality and coherence. *arXiv preprint arXiv:2510.20849*, 2025.
- [4] Dhananjay Ashok and Jonathan May. Language models can predict their own behavior. *Advances in Neural Information Processing Systems*, 38:62708–62739, 2026.
- [5] Jinheon Baek, Sujay Kumar Jauhar, Silviu Cucerzan, and Sung Ju Hwang. Researchagent: Iterative research idea generation over scientific literature with large language models. In

Proceedings of the 2025 Conference of the Nations of the Americas Chapter of the Association for Computational Linguistics: Human Language Technologies (Volume 1: Long Papers), pages 6709–6738, 2025.

- [6] Ananth Balashankar, Ziteng Sun, Jonathan Berant, Jacob Eisenstein, Michael Collins, Adrian Hutter, Jong Lee, Chirag Nagpal, Flavien Prost, Aradhana Sinha, et al. Infalgin: Inference-aware language model alignment. *arXiv preprint arXiv:2412.19792*, 2024.
- [7] Bruce G Buchanan and Edward A Feigenbaum. Dendral and meta-dendral: Their applications dimension. In *Readings in artificial intelligence*, pages 313–322. Elsevier, 1981.
- [8] Ricardo J. G. B. Campello, Davoud Moulavi, and Jörg Sander. Density-based clustering based on hierarchical density estimates. In *Advances in Knowledge Discovery and Data Mining*, pages 160–172. Springer, 2013. doi: 10.1007/978-3-642-37456-2_14.
- [9] Yung-Sung Chuang, Yang Li, Dong Wang, Ching-Feng Yeh, Kehan Lyu, Ramya Raghavendra, James Glass, Lifei Huang, Jason Weston, Luke Zettlemoyer, et al. Meta clip 2: A worldwide scaling recipe. *arXiv preprint arXiv:2507.22062*, 2025.
- [10] Aniket Didolkar, Anirudh Goyal, Nan Rosemary Ke, Siyuan Guo, Michal Valko, Timothy Lillicrap, Danilo Rezende, Yoshua Bengio, Michael Mozer, and Sanjeev Arora. Metacognitive capabilities of llms: An exploration in mathematical problem solving, 2024.
- [11] Anil R. Doshi and Oliver P. Hauser. Generative AI enhances individual creativity but reduces the collective diversity of novel content. *Science Advances*, 10:eadn5290, 2024. doi: 10.1126/sciadv.adn5290.
- [12] Juraj Gottweis, Wei-Hung Weng, Alexander Daryin, Tao Tu, Anil Palepu, Petar Sirkovic, Artiom Myaskovsky, Felix Weissenberger, Keran Rong, Ryutaro Tanno, et al. Towards an AI co-scientist. *arXiv preprint arXiv:2502.18864*, 2025.
- [13] Hojae Han, Seung-won Hwang, Rajhans Samdani, and Yuxiong He. Convcodeworld: Benchmarking conversational code generation in reproducible feedback environments. *arXiv preprint arXiv:2502.19852*, 2025.
- [14] Thomas Hayes, Roshan Rao, Halil Akin, Nicholas J Sofroniew, Deniz Oktay, Zeming Lin, Robert Verkuil, Vincent Q Tran, Jonathan Deaton, Marius Wiggert, et al. Simulating 500 million years of evolution with a language model. *Science*, 387(6736):850–858, 2025.
- [15] Wei Huang, Haotong Qin, Yangdong Liu, Yawei Li, Qinshuo Liu, Xianglong Liu, Luca Benini, Michele Magno, Shiming Zhang, and Xiaojuan Qi. Slim-llm: Saliency-driven mixed-precision quantization for large language models. *arXiv preprint arXiv:2405.14917*, 2024.
- [16] Naman Jain, Alex Gu, Wen-Ding Li, Fanjia Yan, Tianjun Zhang, Sida Wang, Armando Solar-Lezama, Koushik Sen, and Ion Stoica. Livecodebench: Holistic and contamination free evaluation of large language models for code. In *International Conference on Learning Representations*, volume 2025, pages 58791–58831, 2025.
- [17] Lianchen Jia, Chaoyang Li, Qian Houde, Tianchi Huang, Jiangchuan Liu, and Lifeng Sun. Crucible: Quantifying the potential of control algorithms through llm agents. *arXiv preprint arXiv:2510.18491*, 2025.
- [18] Liwei Jiang, Yuanjun Chai, Margaret Li, Mickel Liu, Raymond Fok, Nouha Dziri, Yulia Tsvetkov, Maarten Sap, Alon Albalak, and Yejin Choi. Artificial hivemind: The open-ended homogeneity of language models (and beyond). *arXiv preprint arXiv:2510.22954*, 2025.
- [19] Priyanka Kargupta, Shuhaib Mehri, Dilek Hakkani-Tur, and Jiawei Han. Sparking scientific creativity via LLM-driven interdisciplinary inspiration. *arXiv preprint arXiv:2603.12226*, 2026.
- [20] Simran Kaur, Simon Park, Anirudh Goyal, and Sanjeev Arora. Instruct-skillmix: A powerful pipeline for llm instruction tuning. In *International Conference on Learning Representations*, 2025. doi: 10.48550/arXiv.2408.14774.

- [21] Pat Langley. *Scientific discovery: Computational explorations of the creative processes*. MIT press, 1987.
- [22] Pat Langley. Integrated systems for computational scientific discovery. In *Proceedings of the AAAI Conference on Artificial Intelligence*, volume 38, pages 22598–22606, 2024.
- [23] Douglas B. Lenat. Automated theory formation in mathematics. In *Proceedings of the 5th International Joint Conference on Artificial Intelligence - Volume 2, IJCAI’77*, page 833–842, San Francisco, CA, USA, 1977. Morgan Kaufmann Publishers Inc.
- [24] Zhenyu Li, Yike Zhang, Tengyu Pan, Yutao Sun, Zhichao Duan, Junjie Fang, Rong Han, Zixuan Wang, and Jianyong Wang. Focusllm: Precise understanding of long context by dynamic condensing. In *Proceedings of the 63rd Annual Meeting of the Association for Computational Linguistics (Volume 1: Long Papers)*, pages 31087–31101, 2025.
- [25] Chris Lu, Samuel Holt, Claudio Fanconi, Alex Chan, Jakob Foerster, Mihaela van der Schaar, and Robert Lange. Discovering preference optimization algorithms with and for large language models. *Advances in Neural Information Processing Systems*, 37:86528–86573, 2024.
- [26] Chris Lu, Cong Lu, Robert Tjarko Lange, Jakob Foerster, Jeff Clune, and David Ha. The AI scientist: Towards fully automated open-ended scientific discovery. *arXiv preprint arXiv:2408.06292*, 2024.
- [27] Maria Marina, Nikolay Ivanov, Sergey Pletenev, Mikhail Salnikov, Daria Galimzianova, Nikita Krayko, Vasily Kononov, Alexander Panchenko, and Viktor Moskvoretskii. Llm-independent adaptive rag: Let the question speak for itself. In *Proceedings of the 2025 Conference on Empirical Methods in Natural Language Processing*, pages 8708–8720, 2025.
- [28] Leland McInnes, John Healy, and Steve Astels. hdbscan: Hierarchical density based clustering. *Journal of Open Source Software*, 2(11):205, 2017. doi: 10.21105/joss.00205.
- [29] Viacheslav Meshchaninov, Egor Chimbulatov, Alexander Shabalin, Aleksandr Abramov, and Dmitry Vetrov. Cosmos: Compressed and smooth latent space for text diffusion modeling. *arXiv preprint arXiv:2506.21170*, 2025.
- [30] Alexander Novikov, Ngân Vũ, Marvin Eisenberger, Emilien Dupont, Po-Sen Huang, Adam Zsolt Wagner, Sergey Shirobokov, Borislav Kozlovskii, Francisco JR Ruiz, Abbas Mehrabian, et al. Alphaevolve: A coding agent for scientific and algorithmic discovery. *arXiv preprint arXiv:2506.13131*, 2025.
- [31] OpenReview. OpenReview Reviews for Cosmos: Compressed and Smooth Latent Space for Text Diffusion Modeling. <https://openreview.net/forum?id=Rv6Lz84F1Z>, 2025. NeurIPS 2025 anonymous reviews and meta-review; accessed May 6, 2026.
- [32] Marissa Radensky, Simra Shahid, Raymond Fok, Pao Siangliulue, Tom Hope, and Daniel S Weld. Scideator: Human-llm scientific idea generation grounded in research-paper facet recombination. *arXiv preprint arXiv:2409.14634*, 2024.
- [33] Bernardino Romera-Paredes, Mohammadamin Barekatin, Alexander Novikov, Matej Balog, M Pawan Kumar, Emilien Dupont, Francisco JR Ruiz, Jordan S Ellenberg, Pengming Wang, Omar Fawzi, et al. Mathematical discoveries from program search with large language models. *Nature*, 625(7995):468–475, 2024.
- [34] Tim Schopf and Michael Färber. Is this idea novel? an automated benchmark for judgment of research ideas. In *Proceedings of the Language Resources and Evaluation Conference (LREC)*, 2026. URL <https://arxiv.org/abs/2603.10303>.
- [35] Haozhan Shen, Kangjia Zhao, Tiancheng Zhao, Ruochen Xu, Zilun Zhang, Mingwei Zhu, and Jianwei Yin. Zoomeye: Enhancing multimodal llms with human-like zooming capabilities through tree-based image exploration. In *Proceedings of the 2025 Conference on Empirical Methods in Natural Language Processing*, pages 6613–6629, 2025.

- [36] Feng Shi and James Evans. Surprising combinations of research contents and contexts are related to impact and emerge with scientific outsiders from distant disciplines. *Nature Communications*, 14(1):1641, 2023.
- [37] Chenglei Si, Diyi Yang, and Tatsunori Hashimoto. Can llms generate novel research ideas? a large-scale human study with 100+ nlp researchers. *arXiv preprint arXiv:2409.04109*, 2024.
- [38] Chenglei Si, Tatsunori Hashimoto, and Diyi Yang. The ideation-execution gap: Execution outcomes of LLM-generated versus human research ideas. In *The Fourteenth International Conference on Learning Representations*, 2026. URL <https://openreview.net/forum?id=F11p816Puy>.
- [39] Jamshid Sourati and James A. Evans. Accelerating science with human-aware artificial intelligence. *Nature Human Behaviour*, 7:1682–1696, 2023. doi: 10.1038/s41562-023-01648-z. URL <https://arxiv.org/abs/2306.01495>.
- [40] Robin Staab, Mark Vero, Mislav Balunovic, and Martin Vechev. Language models are advanced anonymizers. In *The Thirteenth International Conference on Learning Representations*, 2025.
- [41] Noy Sternlicht and Tom Hope. Chimera: A knowledge base of idea recombination in scientific literature. *arXiv preprint arXiv:2505.20779*, 2025.
- [42] Wei Sun, Qianlong Du, Fuwei Cui, and Jiajun Zhang. An efficient and precise training data construction framework for process-supervised reward model in mathematical reasoning. In *Proceedings of the 63rd Annual Meeting of the Association for Computational Linguistics (Volume 1: Long Papers)*, pages 4292–4305, 2025.
- [43] Amos Tversky and Daniel Kahneman. Availability: A heuristic for judging frequency and probability. *Cognitive psychology*, 5(2):207–232, 1973.
- [44] Ashish Vaswani, Noam Shazeer, Niki Parmar, Jakob Uszkoreit, Llion Jones, Aidan N. Gomez, Lukasz Kaiser, and Illia Polosukhin. Attention is all you need. *CoRR*, abs/1706.03762, 2017. URL <http://arxiv.org/abs/1706.03762>.
- [45] Qingyun Wang, Doug Downey, Heng Ji, and Tom Hope. Scimon: Scientific inspiration machines optimized for novelty. In *Proceedings of the 62nd Annual Meeting of the Association for Computational Linguistics (Volume 1: Long Papers)*, pages 279–299, 2024.
- [46] Yidong Wang, Qi Guo, Wenjin Yao, Hongbo Zhang, Xin Zhang, Zhen Wu, Meishan Zhang, Xinyu Dai, Min Zhang, Qingsong Wen, et al. Autosurvey: Large language models can automatically write surveys. *Advances in neural information processing systems*, 37:115119–115145, 2024.
- [47] Cong Wei, Zheyang Xiong, Weiming Ren, Xeron Du, Ge Zhang, and Wenhui Chen. Omniedit: Building image editing generalist models through specialist supervision. In *International Conference on Learning Representations*, volume 2025, pages 259–271, 2025.
- [48] Shitao Xiao, Zheng Liu, Peitian Zhang, and Niklas Muennighoff. C-pack: Packaged resources to advance general chinese embedding, 2023.
- [49] Frank F Xu, Uri Alon, Graham Neubig, and Vincent Josua Hellendoorn. A systematic evaluation of large language models of code. In *Proceedings of the 6th ACM SIGPLAN international symposium on machine programming*, pages 1–10, 2022.
- [50] Dingli Yu, Simran Kaur, Arushi Gupta, Jonah Brown-Cohen, Anirudh Goyal, and Sanjeev Arora. Skill-mix: a flexible and expandable family of evaluations for ai models, 2023.
- [51] Leixin Zhang, Steffen Eger, Yinjie Cheng, Weihe Zhai, Jonas Belouadi, Fahimeh Moafian, and Zhixue Zhao. Scimage: How good are multimodal large language models at scientific text-to-image generation? In *International Conference on Learning Representations*, volume 2025, pages 6923–6948, 2025.
- [52] Yanzhe Zhang, Tao Yu, and Diyi Yang. Attacking vision-language computer agents via pop-ups. In *Proceedings of the 63rd Annual Meeting of the Association for Computational Linguistics (Volume 1: Long Papers)*, pages 8387–8401, 2025.

- [53] Zhen Zhang and James Evans. Language model perplexity predicts scientific surprise and transformative impact. *arXiv preprint arXiv:2509.05591*, 2025. URL <https://arxiv.org/abs/2509.05591>.
- [54] Xinran Zhao, Boyuan Zheng, Chenglei Si, Haofei Yu, Ken Liu, Runlong Zhou, Ruochen Li, Tong Chen, Xiang Li, Yiming Zhang, et al. The ramon llull’s thinking machine for automated ideation. *arXiv preprint arXiv:2508.19200*, 2025.
- [55] Yi Zhao, Yajuan Peng, Nguyen Cam-Tu, Zuchao Li, Xiaoliang Wang, Hai Zhao, and Xiaoming Fu. Smallkv: Small model assisted compensation of kv cache compression for efficient llm inference. *Advances in Neural Information Processing Systems*, 38:48637–48665, 2026.
- [56] Wenqiao Zhu, Ji Liu, Rongjunchen Zhang, Haipang Wu, and Yulun Zhang. Carft: Boosting llm reasoning via contrastive learning with annotated chain-of-thought-based reinforced fine-tuning. In *Proceedings of the 2025 Conference on Empirical Methods in Natural Language Processing*, pages 5933–5948, 2025.

A Implementation Details

Algorithm 1 Alien Science Sampling Pipeline

- 1: **Input:** corpus of papers \mathcal{P} , researcher profiles \mathcal{R}
 - 2: // *Representation*
 - 3: Extract conceptual units from each paper; cluster into atom vocabulary \mathcal{V}
 - 4: Map each paper to its expressed atoms \rightarrow atom sequences $\{S_p\}_{p \in \mathcal{P}}$
 - 5: // *Model training*
 - 6: Train coherence model C on atom sequences from papers
 - 7: Train availability model A on atom sets grouped by researcher profile
 - 8: // *Alien sampling*
 - 9: Sample N candidate sequences from C at temperature τ (or by random sampling from the space of sets of atoms)
 - 10: Score each candidate by coherence $C(S)$ and unavailability $U(S) = -A(S)$
 - 11: Standardize both scores within the candidate pool
 - 12: Select candidates with high combined coherence–unavailability score
 - 13: **Output:** top-scoring candidates as alien research directions
-

A.1 Data Collection

We construct the corpus in two stages. First, we collect papers from selected ML and NLP venues using OpenReview and DBLP metadata, with Semantic Scholar metadata used to fill missing abstracts, keywords, and PDF links. Second, we apply the LLM field filter over title, abstract, and keywords, retaining papers that match at least one of these metadata fields. This yields 16,068 papers with usable PDF URLs. Table 2 summarizes the selection procedure; Table 3 gives the exact venue-year distribution.

Field	Value
Metadata sources	OpenReview, DBLP, Semantic Scholar
Selection filter	LLM match in title, abstract, or keywords
Venues	NeurIPS, EMNLP, ACL, ICLR, ICML, AAAI, COLM, NAACL, IJCAI
Years	2017–2025
Total papers	16,068

Table 2: Corpus construction summary.

Venue	2017	2018	2019	2020	2021	2022	2023	2024	2025	Total
NeurIPS	0	3	12	19	50	115	348	955	1,720	3,222
EMNLP	12	32	0	0	0	272	500	954	1,253	3,023
ACL	9	18	47	106	0	173	413	636	1,221	2,623
ICLR	16	27	19	55	85	108	285	559	1,395	2,549
ICML	2	4	6	8	15	32	110	536	956	1,669
AAAI	2	13	12	40	52	66	95	307	758	1,345
COLM	0	0	0	0	0	0	0	279	386	665
NAACL	0	10	0	0	90	124	0	306	0	530
IJCAI	4	3	9	6	11	26	34	118	231	442
Total	45	110	105	234	303	916	1,785	4,650	7,920	16,068

Table 3: Distribution of LLM-filtered papers by venue and year. Zero entries indicate years with no papers from that venue in the filtered database.

A.2 Model usage

Gemini 3 Flash was used for the atomization pipeline: reading papers, producing compressed summaries, extracting conceptual units, evaluating candidate clusters, and naming the resulting clusters/atoms. For the LLM baselines, Gemini 3.1 Pro and Claude Opus 4.7 were prompted to select novel yet feasible atom combinations from the atom vocabulary. After decoder experimentation, Claude Opus 4.7 was used to reconstruct atom combinations into natural-language research ideas. Gemini 3.1 Pro was used as the LLM-as-judge for reviewing generated ideas.

A.3 Paper Compression

Each paper is distilled into a high-signal “blog post” summary, approximately 2 pages in length. This compression specifically targets methodology over results, removing formatting noise, verbose citations, and granular experimental details while preserving the core research contribution in accessible prose.

A.4 Conceptual Unit Extraction

Conceptual units are extracted from compressed blog posts using an LLM. The number of units per paper is flexible rather than fixed. Each unit must satisfy three quality criteria:

- **Self-standing:** interpretable without the original paper context
- **Recombinable:** can meaningfully pair with units from other papers
- **No dangling references:** avoids paper-specific notation or undefined terms

A.5 Atom Clustering

We cluster conceptual units into a shared vocabulary of transferable atoms using BGE embeddings, UMAP dimensionality reduction, and HDBSCAN. HDBSCAN’s hyperparameters are selected by the LLM-as-judge clustering evaluation described in Section B.

Metric	Value
Input conceptual units	82,255
Initial HDBSCAN clusters	273
Initial noise units	62.8%
Selected coverage after reassignment	80%
Mean atoms per paper before reassignment	1.65
Mean atoms per paper at selected coverage	3.38
Clustering algorithm	UMAP + HDBSCAN
Embedding model	BAAI/bge-large-en-v1.5

Each cluster is summarized by an LLM into a canonical atom description representing the shared concept. Units initially labeled as noise are incrementally reassigned to their nearest cluster centroid, ordered by embedding similarity, until the selected 80% coverage point is reached. This reassignment is used only to construct denser paper–atom sequences for training the coherence and availability models. It does not change the atom descriptions, and it is not used as evidence that reassigned units exactly match the target atom.

Paper and author coverage over atoms. The resulting atom space is broad but unevenly supported. Figure 6 shows the number of distinct papers contributing to each cluster. Across the 273 clusters, support ranges from 7 to 604 papers with standard deviation 92.7. Most clusters are supported by a few dozen papers: the median cluster appears in 44 papers, and the bulk of clusters draw from roughly 20–50 papers. The mean is higher, 81.1 papers per cluster, because a long tail of large cross-cutting clusters captures widely reused methodological motifs that appear across many subareas.

The author side has a similar heavy-tailed structure. The median author node covers only 4 atoms, but the broadest author node covers 145 of 273 atoms; the top 10 author nodes collectively cover 89.0% of the atom universe. These broad profiles are not merely large atom sets: they are also socially well-connected. Figure 7 shows that atom coverage, distinct coauthor degree, and publication count are associated. This matters for availability modeling because a single broad author can connect

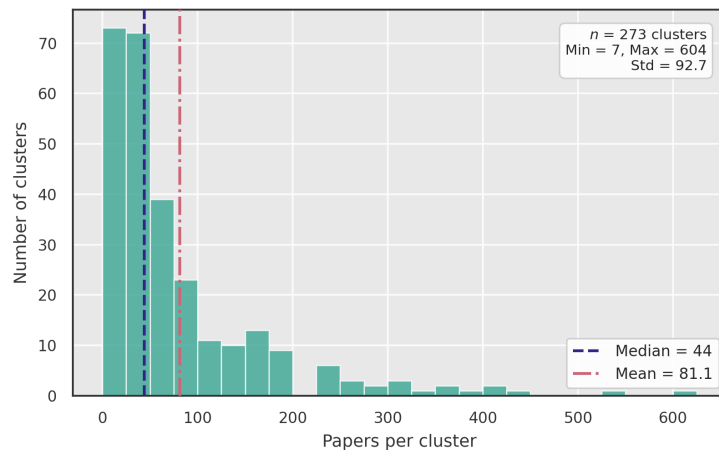


Figure 6: Distribution of papers per atom cluster. Most atom clusters are supported by tens of papers, while a long tail of broad, cross-cutting clusters pulls the mean (81.1) above the median (44).

otherwise distant regions of the atom space, even when no broader community independently supports the combination.

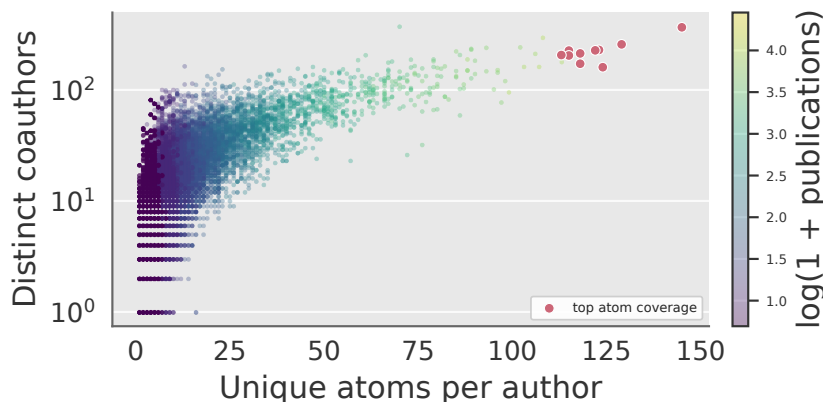


Figure 7: Author connectivity is coupled to atom coverage. Each point is an author node, positioned by unique atom coverage and distinct coauthor degree; color encodes $\log(1 + \text{publications})$, and red points mark the top ten authors by atom coverage. The association shows that broad author profiles are also socially well connected, so individual prolific authors can bridge distant regions of the atom space.

A.6 Training Data

Both learned models use the 80% coverage atom representation described in Section B. We summarize the derived training records here rather than repeating the full venue-year corpus distribution from Table 3. The training JSONL files contain atom IDs and entity IDs, but not venue or year fields, so the quantities below describe the actual model inputs.

Coherence records. The coherence dataset contains paper-level atom sequences for papers with at least two assigned atoms. From 16,068 papers with clustered atom information, 15,203 satisfy this minimum-length filter and 817 are skipped. Each included paper contributes ten serialized sequence variants, producing 152,030 coherence records split 90/10 into 136,827 training records and 15,203 validation records. Atom lengths below exclude the beginning- and end-of-sequence tokens. At the paper level, sequences contain 3.50 atoms on average: 18.3% have length 2, 33.2% length 3, 31.2% length 4, 14.5% length 5, and 2.8% length 6–8.

Availability records. The availability dataset is built from author atom repertoires. An author is included if their profile contains at least two atoms; this retains 25,722 of 26,462 author profiles. Each record follows the subset-complement schema: the set tower receives a positive query subset Q_i of length 2–4, while the author tower receives the remaining profile atoms $R_i \setminus Q_i$. This prevents direct overlap between the two towers for the matched pair. Dataset generation produces 23,167,856 subset-complement records after rejecting 1,365,070 duplicate records. The training loader drops the small number of records with an empty complement, leaving 23,154,105 usable records: 20,838,702 for training and 2,315,403 for validation. The validation split is example-level rather than author-disjoint, so it measures held-out subset-complement pairs rather than retrieval for entirely unseen authors.

Quantity	Coherence data	Availability data
Training objective	Next-atom prediction	Author–set contrastive retrieval
Training records used	136,827	20,838,702
Validation records used	15,203	2,315,403
Source entities	15,203 papers	25,722 authors
Positive input length	Mean 3.50; median 3; p90 5; max 8	Mean 3.79; median 4; p90 4; max 4
Author-tower input length	–	Mean 26.53; median 24; p90 46; max 111
Vocabulary size	273 atoms	273 atoms
Random seed	42	42

Table 4: Training-record characteristics for the coherence and availability models. Lengths count atom IDs, excluding special sequence tokens for coherence. Availability statistics are computed after dropping empty-complement records, matching the records consumed by the two-tower loader.

A.7 Model Training

A.7.1 Coherence Model.

We train a causal transformer where atoms serve as discrete tokens in a vocabulary of 273. These atoms were identified using the clustering selection procedure described in Section B. Training uses autoregressive next-atom prediction on ordered atom sequences derived from papers, where atom order follows the narrative structure of the compressed blog post. The coherence model is trained on the 80% coverage atom representation with the run settings and default architecture details in Table 5.

Parameter	Value
Epochs	30
Batch size	64
Gradient accumulation steps	2
Effective batch size	128
Learning rate	1×10^{-4}
Warmup steps	1,000
Weight decay	0.01
Maximum sequence length	32
Model type	Decoder-only causal Transformer
Vocabulary size	274 tokens
Hidden size	768
Transformer layers	6
Attention heads	12
Feed-forward hidden size	3,072
Dropout	0.1
Parameters	42.8M

Table 5: Run settings and architecture details for the coherence transformer. Architecture values not passed explicitly in the command use the training script defaults. Vocabulary size is 273 atom tokens plus a shared BOS/EOS token.

A.7.2 Order sensitivity diagnostic.

Because the coherence model is autoregressive, a single ordered serialization of an atom set can receive a different score from another ordering of the same atoms. We therefore measure order sensitivity by scoring every permutation of the same unordered k -atom set and computing the standard deviation of the resulting coherence scores. We compare this within-set order variation to the between-category separation among exact real-paper atom sets, uniformly random atom sets, and pairwise-disjoint uncoherent atom sets. For real-paper coherent sets, the average permutation standard deviation is 0.37 for $k = 3$ and 0.63 for $k = 4$. This is much smaller than the coherent–random mean score gaps (3.52 for $k = 3$, 4.18 for $k = 4$) and the coherent–uncoherent gaps (4.55 for $k = 3$, 5.26 for $k = 4$). Thus, although single-order coherence scores are not exactly order-invariant, the coherent-set signal is robust relative to random and deliberately uncoherent baselines.

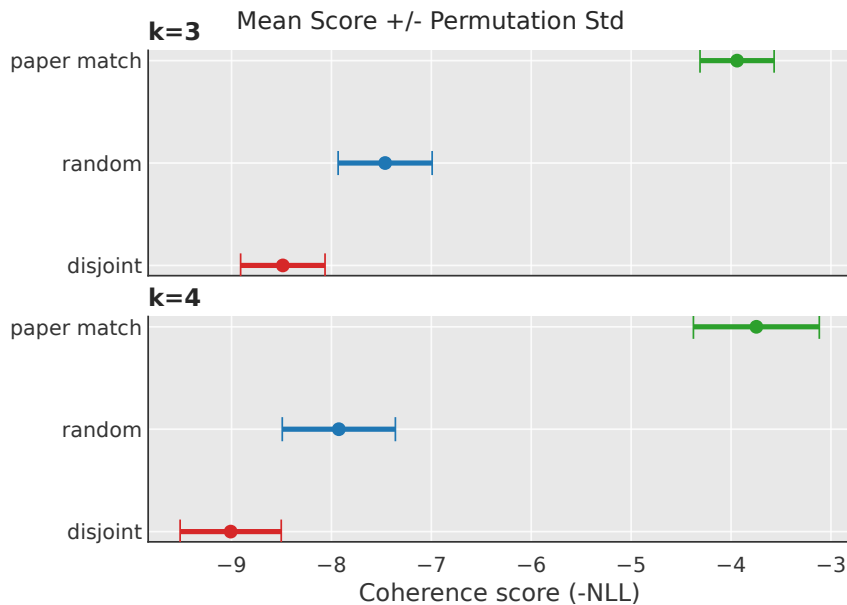


Figure 8: Order sensitivity of coherence scores. Points show the mean coherence score for random, real-paper coherent, and pairwise-disjoint uncoherent atom sets; horizontal bars show ± 1 standard deviation across permutations of the same atom set. Scores are $-NLL$, so higher is more coherent. Although scores vary with atom order, the permutation-induced variation is small relative to the separation between real-paper coherent sets and the random/uncoherent baselines.

A.7.3 Availability Model.

We train a dual-encoder contrastive model that scores compatibility between an author and a candidate atom set. The author encoder represents the author’s known atom repertoire, while the set encoder represents the candidate atoms with a bidirectional Transformer. At inference, low similarity to the nearest author community indicates low cognitive availability. The final availability model uses the settings in Table 6.

A.8 Availability Architecture Comparison

Availability is the part of the pipeline where the modeling choice matters most. A coherence model asks whether atoms form a plausible paper. An availability model asks a different question: whether an existing researcher community is positioned to produce the combination. We therefore compare two availability objectives using the same atom vocabulary and matched $k = 3$ evaluation pools: an author-agnostic density estimator trained with random negatives, and the author-conditioned dual encoder used in the sampler.

Evaluation protocol. We use two complementary evaluations. The broad evaluation compares three pools: *paper-supported* triplets that appear together in a paper; *author-only* triplets covered by at least

Parameter	Value
Epochs	100
Batch size	4,096
Gradient accumulation steps	1
Effective batch size	4,096
Learning rate	5×10^{-4}
Warmup steps	2,000
Weight decay	0.03
Maximum sequence length	128
Hidden size	512
Transformer layers	6
Attention heads	8
Maximum logit scale	30
Compilation	Enabled

Table 6: Training settings for the dual-encoder availability model.

one author profile but not observed in one paper; and *unavailable*, or zero-support, random triplets with no author support. The targeted trap evaluation asks whether a model over-rates combinations with weak community evidence. Here *community-supported* triplets have many supporting authors but no single paper, while *prolific-only* triplets have no paper support and are covered only by one or two broad author profiles. We report AUC-ROC because availability is used as a rank signal: AUC 0.5 means the model cannot order two pools, while higher values mean the positive pool receives higher availability scores. We also report Spearman correlations with corpus statistics as diagnostics, not performance metrics; they show whether a model mostly tracks paper evidence, author breadth, nearest-paper similarity, or atom popularity.

Density estimator with random negatives. The density-estimator baseline uses the same unordered set interface as the set side of the dual encoder, but removes the author tower. Let $f_\theta(S) \in \mathbb{R}$ be the scalar score for atom set S , computed by embedding the atom IDs, applying a bidirectional Transformer with no positional embeddings or causal mask, mean-pooling over non-padding atoms, and passing the pooled vector through an MLP. For each observed positive set S_i^+ , the training loader samples K negative sets $S_{i1}^-, \dots, S_{iK}^-$ with the same cardinality as S_i^+ . Negative atoms are drawn independently from the empirical atom-frequency distribution $q(a)$, so $S_{ik}^- \sim q^{|S_i^+|}$. The model is trained by classifying the positive set against its random negatives:

$$\mathcal{L}_i = -\log \frac{\exp(f_\theta(S_i^+)/\tau)}{\exp(f_\theta(S_i^+)/\tau) + \sum_{k=1}^K \exp(f_\theta(S_{ik}^-)/\tau)}.$$

The implementation forms these logits as $[f_\theta(S_i^+), f_\theta(S_{i1}^-), \dots, f_\theta(S_{iK}^-)]/\tau$, clips them to $[-30, 30]$, and applies cross-entropy with the positive set as class zero. Under the noise-contrastive interpretation of this objective, the learned score estimates a density ratio, increasing with $\log p_{\text{data}}(S) - \log p_{\text{noise}}(S)$, where p_{noise} is induced by the frequency-weighted random sampler. This makes the model strong at separating real-looking combinations from unavailable random controls. However, it has no explicit author input. As a result, it estimates global set familiarity rather than cognitive availability: it cannot answer “available to whom”, and it almost completely fails to distinguish paper-supported triplets from author-only triplets (AUC 0.499).

Dual-encoder availability. The final model keeps the set encoder but adds a separate author encoder. Training pairs a query subset Q_i with the complement of the same author’s repertoire, $R_i \setminus Q_i$, so the task cannot be solved by literal atom overlap. The contrastive objective asks whether the query set retrieves the right author profile and whether the profile retrieves the right query set. At inference, we score a candidate against all author profiles and aggregate the top 10 similarities by their median. This makes availability a community-compatibility score rather than a single-author bridge.

Table 7 shows the main discrimination tests. The selected model is not chosen because it wins every scalar metric. The density estimator distinguishes available-looking sets from unavailable sets, but collapses the distinction between paper-level and author-only evidence. The dual encoder gives the strongest paper-versus-author-only separation and the only retrieval target that preserves the meaning of “available to a community.”

Model	Conditioning	Paper > unav.	Author-only > unav.	Paper > author-only
Density estimator	Random negatives	0.982	0.983	0.499
Dual encoder	Author-set compatibility	0.997	0.977	0.797

Table 7: AUC-ROC for neural availability objectives. The density estimator recognizes available-looking sets, but without author conditioning it does not separate paper support from author-only support.

The targeted trap diagnostic in Table 8 asks whether a model rates prolific-only triplets as available. The density estimator partially falls into this failure mode: 5.3% of its top availability quartile comes from prolific-only directions, and its community-versus-prolific AUC is much lower than the dual encoder. This is the expected limitation of random-negative training: once a set looks plausible globally, the model has no author-conditioned evidence for deciding whether support comes from a real community or only from broad individual profiles. The dual encoder is selected because it rejects this trap while making availability explicitly author-conditioned.

Model	Community > prolific-only	Paper > prolific-only	Prolific-only in top quartile
Density estimator	0.863	0.925	5.3%
Dual encoder	0.999	1.000	0.0%

Table 8: Prolific-author trap diagnostic for neural availability objectives. Prolific-only triplets have no paper support and are covered only by one or two broad author profiles. The density estimator is more permissive on this pool; the dual encoder rejects these directions while preserving author-conditioned retrieval.

Overall, the density estimator is a useful sanity check: random-negative training confirms that atom sets contain enough signal to distinguish plausible combinations from unsupported controls. But that objective does not match the construct of cognitive availability. Our sampler needs a score for whether a direction is reachable by an existing researcher community, and this requires conditioning on researcher profiles. We therefore use the dual encoder as the final availability model: it retains strong discrimination against unavailable and prolific-only controls, while supplying the retrieval evidence needed to interpret availability as support from a community of researchers.

A.9 Atom-Author Hypergraph Comparison

The most important structured baseline is the Sourati–Evans human-aware science hypergraph [39]. We test whether this graph-based signal transfers to our availability problem in a dense AI collaboration graph. We use the same atom universe as the dual encoder and the same deterministic $k = 3$ candidate pools. Availability asks whether a direction is supported by a plausible researcher community, not merely whether a short social path can connect its atoms.

Hypergraph construction and default setting. We construct a publication hypergraph with atom and author nodes. The resulting graph contains 273 atom nodes, 46,329 author nodes, and 16,068 publication hyperedges. Each hyperedge connects the atoms and authors associated with one article. Hyperedges contain 3.38 atoms and 5.98 authors on average. We then learn atom embeddings from Sourati–Evans-style author–atom random walks and score a candidate atom set by mean pairwise cosine similarity in the learned availability embedding.

Our main atom-author hypergraph baseline follows the default walk balance described by Sourati and Evans [39]: $\alpha = 1$, giving equal total sampling weight to atom/material nodes and author nodes after a hyperedge is selected. We adapt their 250,000-walk protocol to our atom vocabulary by using 916 walks per atom, for 250,068 total walks, truncated at length 20. We keep the Word2Vec settings fixed across all alpha values: 128 dimensions, context window 8, 30 epochs, 5 negative samples, and learning rate $0.025 \rightarrow 0.0001$.

The balanced atom-author hypergraph default is a strong baseline, but the availability-only metrics isolate a clear failure mode. The dual encoder ranks community-supported directions above prolific-only bridges, zero-support controls, and random controls with near-perfect AUC. The hypergraph also detects community support at $\alpha = 1$, but its high-scoring region contains substantially more

Method	Comm. > prolific	Comm. > zero	Comm. > random	Trap/noise top Q
Dual encoder	0.999	0.999	0.980	6.0%
Atom-author W2V, $\alpha = 1.0$ default	0.953	0.960	0.910	24.6%
Atom-author W2V, $\alpha = 0.5$	0.844	0.840	0.757	50.6%
Atom-author W2V, $\alpha = 0.1$	0.610	0.579	0.503	76.6%

Table 9: Availability diagnostics for the dual encoder and atom-author hypergraph baselines. Each AUC asks whether the method ranks community-supported triplets above a specific negative control: prolific-only bridges, zero-support triplets, or random triplets. Trap/noise denotes the fraction of the highest-scoring quartile that is prolific-only, zero-support, or random.

trap/noise candidates. Lower alpha values increasingly overweight author-mediated transitions and degrade all three community-discrimination tests.

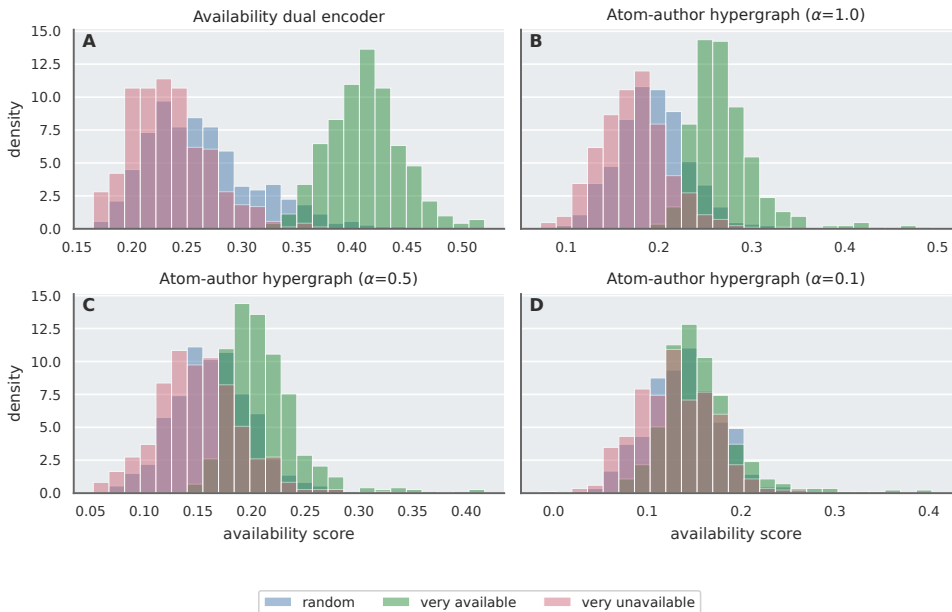


Figure 9: Availability score distributions on identical support-controlled $k = 3$ candidate pools show that the dual encoder separates community-supported directions from zero-support and random controls more clearly. The atom-author hypergraph is also less collapsed at $\alpha = 1$, whereas lower α values cause the three distributions to increasingly overlap.

Alpha ablation. The Sourati-Evans walk parameter α controls the balance between atom/material and author exploration after a publication hyperedge is sampled. In this implementation, atom candidates receive total weight α and author candidates receive total weight 1. Thus $\alpha = 1$ is balanced, while smaller values overweight author-mediated transitions. Figure 12 reruns the hypergraph baseline with matched 250k-walk settings while varying only α .

Why density matters. The AI author-atom graph is extremely dense, with the broad author and coauthorship structure summarized in Section A.5. Starting from an atom, direct publication incidence reaches 55.1% of the atom vocabulary at radius 1 and all atoms by radius 2. Once author nodes are included, the author-mediated graph reaches the full atom vocabulary immediately under the semantic-hop convention (Figure 13). Thus path existence is too weak a signal: many directions are reachable through short social paths even when they are not supported by a coherent author community.

Overall, the atom-author hypergraph is a strong and appropriate structured baseline when run at its balanced default setting. The difference is one of inductive bias. The hypergraph is effective at

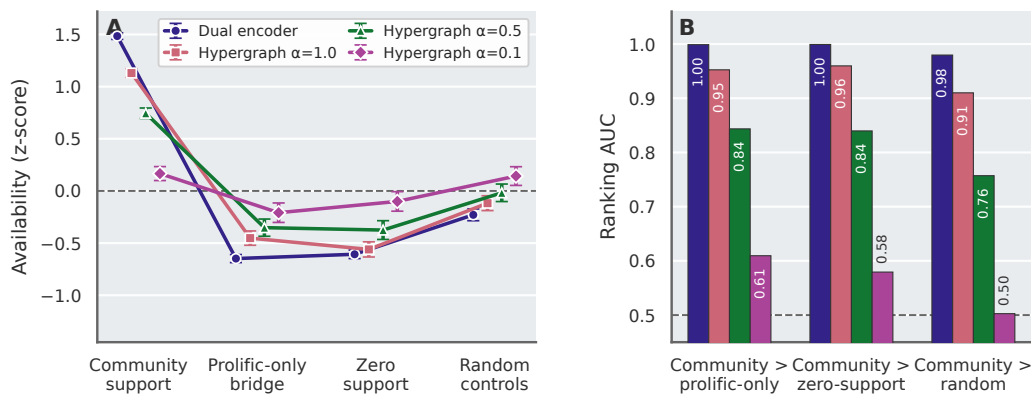


Figure 10: Availability scoring under dense author support. We compare the dual encoder with atom-author walk+Word2Vec hypergraph baselines on matched $k = 3$ atom sets. Hypergraph $\alpha = 1$ is the balanced default; $\alpha = 0.5$ and $\alpha = 0.1$ increasingly overweight author-mediated transitions. Panel A shows mean standardized availability for four author-support regimes. Panel B reports pairwise AUCs: the probability that a community-supported triplet receives a higher score than the named control class.

exploiting publication and author-mediated proximity, but dense author reachability can make unsupported directions look available. The dual encoder instead aggregates similarity across the retrieved author community, so a direction is judged available only when the nearest author neighborhood agrees, not merely when one broad author node bridges the atoms.

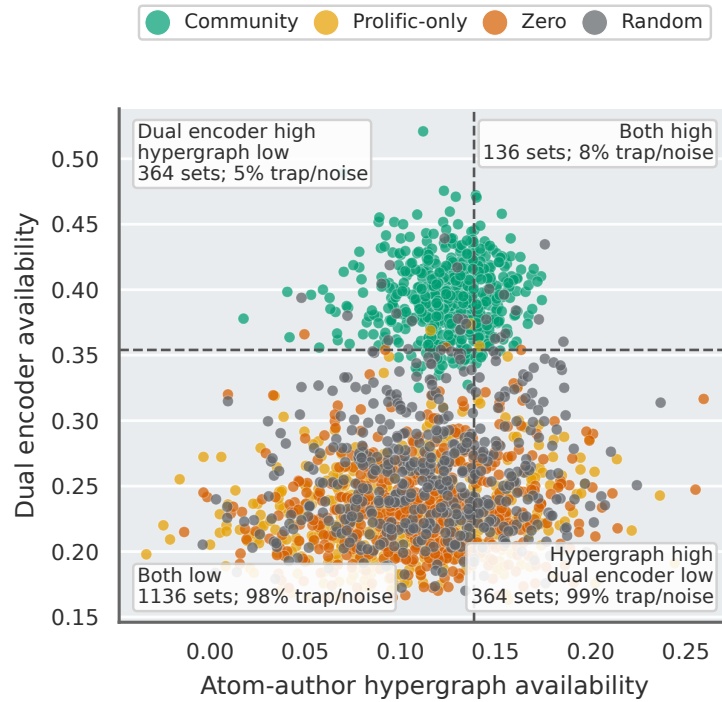


Figure 11: Model-disagreement quadrants for the availability diagnostic pools. Dashed lines mark each method’s top-quartile threshold. The upper-right quadrant contains consensus-available directions; the lower-left contains consensus-low directions. The lower-right quadrant is the critical failure mode for this appendix: directions scored high by the atom-author hypergraph but low by the dual encoder. Its trap/noise rate is much higher because many of these directions are reachable through broad author bridges rather than supported by a coherent author community.

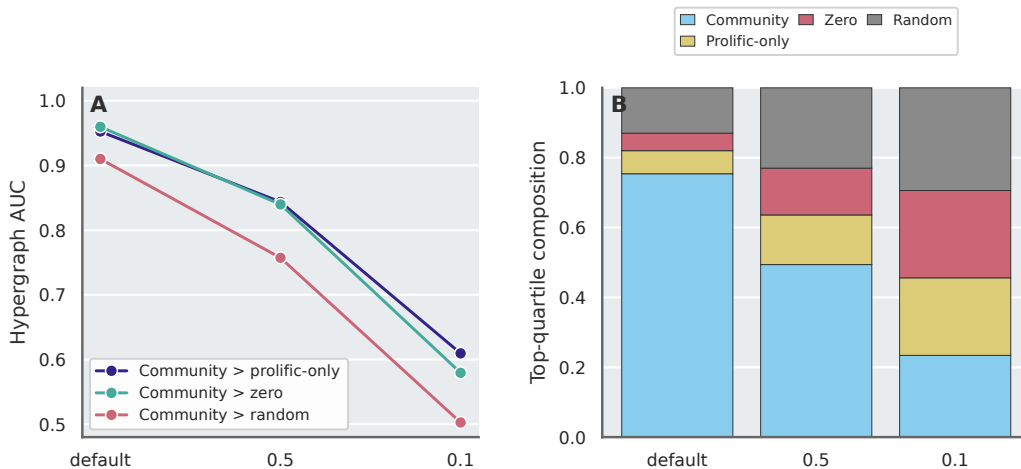


Figure 12: Sensitivity to author/atom walk balance. The balanced atom-author hypergraph default ($\alpha = 1$) is the strongest setting. Panel A reports availability-only AUCs for community-supported triplets against three control classes. Panel B shows that lower alpha values increase the fraction of prolific-only, zero-support, and random candidates in the hypergraph high-scoring region.

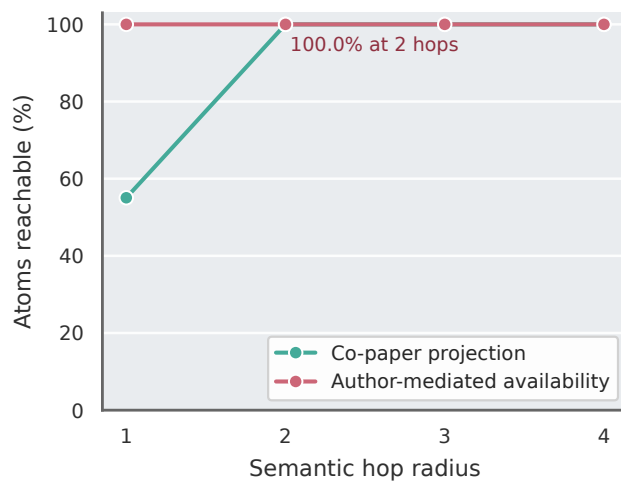


Figure 13: Dense author-mediated paths collapse the atom space. In the shared AI hypergraph, publication incidence already reaches all atoms by two steps, and adding author nodes reaches the full atom universe immediately under the semantic-hop convention. This explains why availability is difficult to infer from graph reachability alone.

A.10 Availability Space for Three-Atom Combinations

Figure 14 shows the availability distribution over the full $k = 3$ candidate space. This diagnostic explains why random recombination is not enough to obtain cognitively unavailable directions in our domain. The LLM literature is dense enough that many uniformly random triples still fall near some author community under the dual encoder. Consequently, the random mean is more available than the Alien $\beta = 0.7$ mean. Low availability is concentrated in a left-tail region of the exhaustive space, so reaching it requires explicit optimization against availability rather than random sampling.

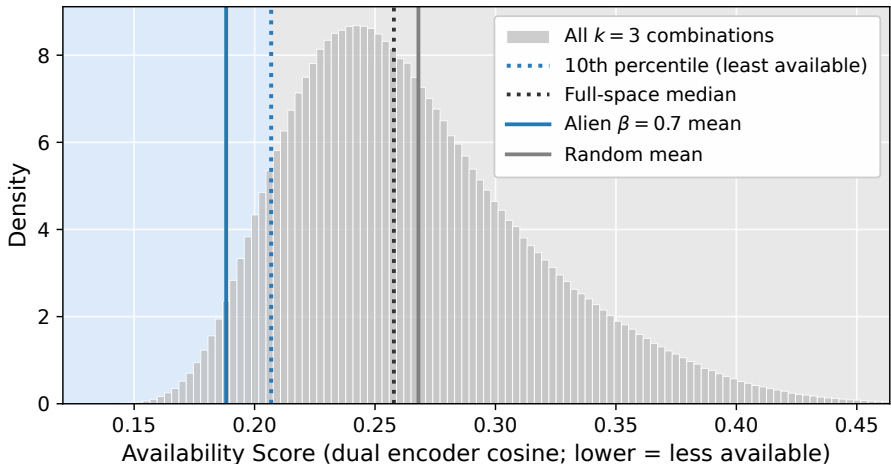


Figure 14: Availability distribution over all possible $k = 3$ atom combinations. Lower scores are less available. The shaded region marks the bottom 10% least-available triples. Random sampling lands closer to the full-space mean, whereas Alien sampling at $\beta = 0.7$ deliberately moves into the less-available tail.

A.11 Sampling Parameters

For $k = 3$ we generate from all possible combinations of our 273 atoms and use the coherence and availability models to search in this space. For $k = 4$, we sample $N = 10,000$ candidate atom sequences from the coherence model at temperature $T = 1$. Coherence is measured by length-normalized log-likelihood under the coherence model, while unavailability is measured as the negative top-community similarity under the availability model. We standardize both scores within the candidate pool and select the top-300 candidates by the combined coherence–unavailability score used in the main text. Each selected atom sequence is reconstructed into a natural language research idea using the reconstruction pipeline described in Section B.

A.11.1 Selecting β

The fusion weight β controls a real trade-off rather than a nuisance hyperparameter: larger values move the sampler toward lower availability, but eventually sacrifice the coherence constraint that distinguishes alien science from random recombination. We therefore selected β before the final baseline comparison using a separate sweep over $\beta \in \{0.0, 0.1, \dots, 1.0\}$. For each atom-set size k , the sweep held the candidate pool fixed and re-ranked the same candidates under each β , selecting the top 300 for reconstruction. For $k = 3$ the sweep exhaustively scored all 3,353,896 triples; for $k = 4$ it scored 52,952 unique sets sampled from 100,000 coherence-model generations. This makes neighboring β values directly comparable: only the fusion weight changes.

The evaluation has two separate components. First, we reconstruct the beta-selected atom sets with each candidate reconstructor. This lets us ask whether decoder capacity changes how much signal can be extracted from the same recombinations. Second, within each reconstructor and each k , we compare beta values by pairwise originality judgments. For every pair of beta methods, the judge sees two reconstructed ideas from the corresponding beta-selected sets and chooses which is the more original recombination; presentation order is randomized, ties count as half wins, and the resulting tournament is summarized with a position-adjusted Bradley–Terry score. We also compare each beta

method against a random baseline. Coherence is not evaluated pairwise: each reconstructed idea is rated independently with a five-level coherence rubric, and we aggregate the per-sample scores for each beta method.

This separation matters because decoder capacity changes the absolute quality of reconstructions but not the basic beta trend. Figure 15 shows that stronger reconstructors, especially Claude Opus 4.7, extract more useful signal from a fixed atom-selection procedure: they produce higher coherence and higher absolute originality across most beta values. At the same time, all reconstructors follow the same qualitative pattern as β increases: originality rises while coherence falls. Figure 16 confirms the reconstructor choice more directly by holding atom sets fixed and running pairwise originality comparisons between decoders. Claude Opus 4.7 wins most head-to-head comparisons against both Gemini 3.1 Pro and Gemini 3 Flash, so we choose β in the same decoder setting used for the main reconstructed outputs: the $k = 3$ Claude Opus 4.7 beta sweep.

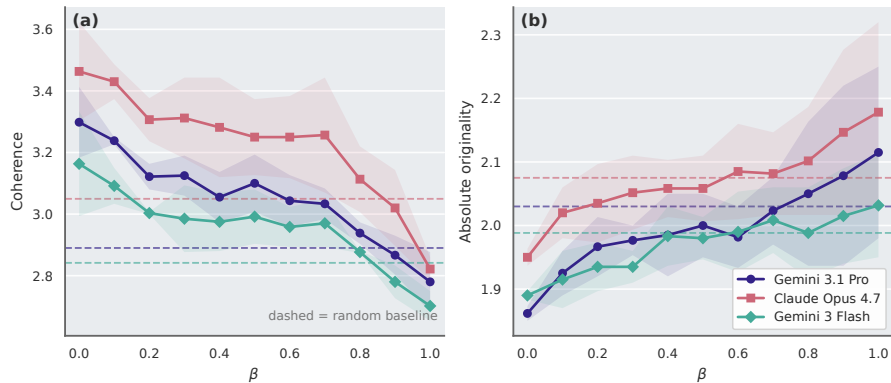


Figure 15: Reconstruction-model capability across beta values. The same beta-selected atom combinations are reconstructed with different decoders. Coherence and absolute originality are rated independently per sample; dashed lines show the random baseline. Stronger reconstructors extract more signal from the same recombinations, but the coherence–originality trend as β changes is similar across decoder capacity.

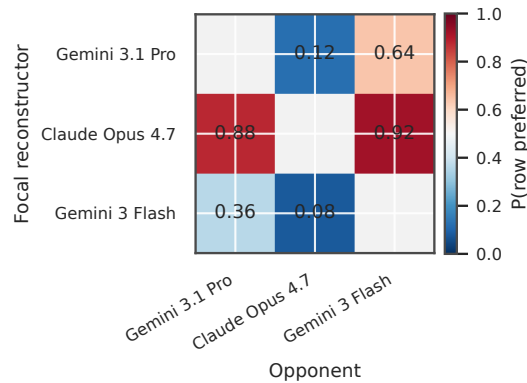


Figure 16: Pairwise originality comparison between reconstructors while holding atom sets fixed. Each cell is the focal reconstructor’s win rate against the opponent. Claude Opus 4.7 is the strongest decoder, so the main beta choice is made in the Claude reconstruction setting.

Figure 17 and Table 10 show the decisive $k = 3$ Claude sweep. We use within-run z -scores so pairwise originality and individually judged coherence are on a common scale. The selection score is 0.67 times position-adjusted pairwise originality plus 0.33 times judged coherence. In the best-reconstructor setting, $\beta = 0.7$ is the best beta under this selection rule. Moving from $\beta = 0.7$ to $\beta = 0.8$ gives a small additional gain in pairwise originality, but it flips coherence from above-average

to below-average and drops the raw coherence score below the random baseline for this run (3.22 vs. 3.32). We therefore choose $\beta = 0.7$ for the rest of the paper.

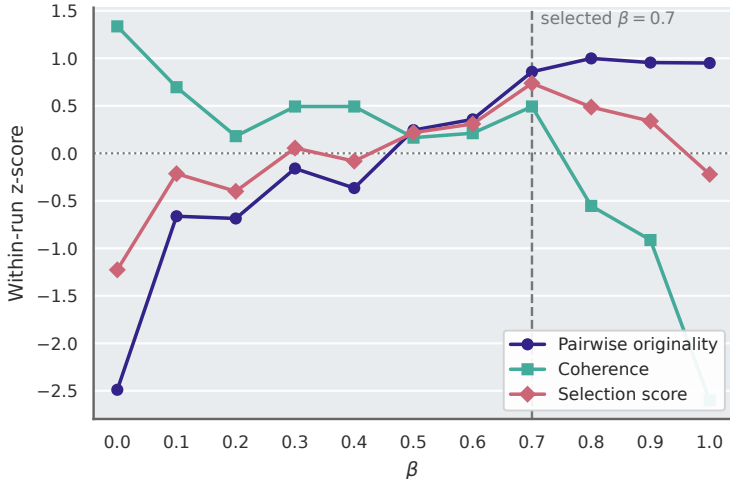


Figure 17: Beta selection for the final $k = 3$ Claude Opus 4.7 setting. Pairwise originality is obtained from beta-versus-beta originality comparisons; coherence is rated independently per reconstructed sample. The selection score combines the two standardized signals, and is maximized at $\beta = 0.7$.

β	Pairwise originality z	Coherence z	Coherence mean	Trade-off
0.6	0.36	0.21	3.38	0.31
0.7	0.86	0.49	3.44	0.74
0.8	1.00	-0.55	3.22	0.49
0.9	0.95	-0.91	3.14	0.34
1.0	0.95	-2.60	2.78	-0.22

Table 10: Beta-selection neighborhood for the final $k = 3$ Claude Opus 4.7 reconstruction setting. Pairwise originality comes from beta-versus-beta originality comparisons; coherence is rated independently per sample. Both are standardized within the beta sweep. The trade-off column is $0.67 \cdot z_{\text{pairwise}} + 0.33 \cdot z_{\text{coherence}}$; $\beta = 0.7$ is best under this criterion. The random baseline’s raw coherence mean in this run is 3.32.

A.12 Decoder stability.

As a diagnostic, we measured how consistently the reconstruction decoder maps a fixed atom combination to text. For each generation method, we sampled five atom combinations and generated five independent reconstructions per combination using Claude Opus 4.7 with the same reconstruction prompt. We embedded the resulting texts and computed pairwise cosine similarity only among reconstructions of the same atom combination. The mean within-idea cosine similarity was 0.902, showing that the decoder is generally stable: repeated decodes usually preserve the same semantic research direction.

However, the distribution also shows that the mapping from atom combinations to reconstructed ideas is not strictly one-to-one. Some reconstruction pairs for the same atom combination have substantially lower similarity, with values near 0.8 and a minimum around 0.76. This suggests that a fixed atom set can support multiple nearby, but meaningfully distinct, research interpretations. Thus, while most exploration in our current pipeline comes from the sampler, the decoder itself can introduce limited semantic variation. Future variants could make this source of diversity explicit by prompting for multiple distinct interpretations of the same atom set or conditioning later reconstructions on previous attempts. In this work, we keep the reconstruction protocol fixed for simplicity and use the first decoded reconstruction for each sampled atom combination.

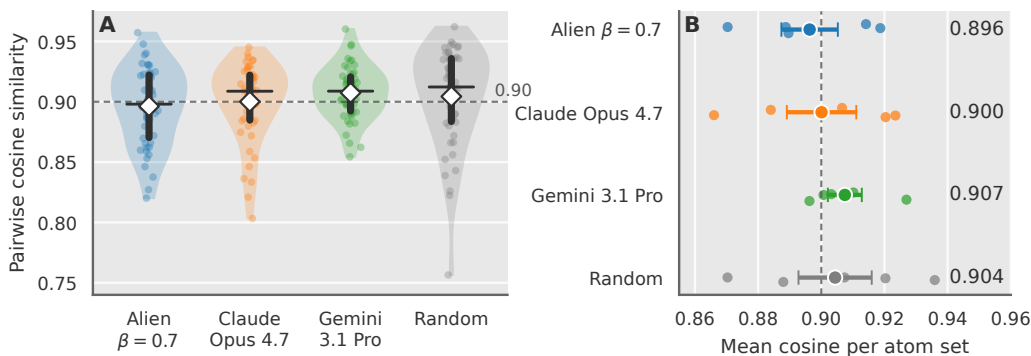


Figure 18: Decoder stability under repeated reconstruction. For each method, five atom combinations were reconstructed five times with Claude Opus 4.7. Panel A shows within-idea pairwise cosine similarities between reconstructions, and Panel B shows atom-combination means with SEM across ideas. The decoder is generally stable, but occasional lower-similarity pairs indicate that a fixed atom combination can admit multiple distinct reconstructions.

A.12.1 Predicting 2025 papers from models trained through 2024

The beta sweep above selects a sampling setting for generating reconstructed research ideas. The main corpus spans 2017–2025, and 2025 is not a small tail split: it contributes 7,920 of the 16,068 collected papers, or 49.3% of the corpus. We therefore ran a separate temporal diagnostic in which the scoring models are trained only on papers up to 2024 and are then asked to recover atom combinations that appear in 2025 papers. This is a deliberately strict backtest: the target is not semantic similarity to a future paper, but exact recovery of its three-atom set.

We trained the coherence model and availability model on the through-2024 datasets and evaluated against 2025 papers in the full corpus. Held-out targets are therefore papers from 2025 that were absent from the training corpus. Among these 2025 papers, there are 2,503 papers with exactly three atoms, corresponding to 2,477 unique three-atom sets. We exhaustively enumerated all $\binom{273}{3} = 3,353,896$ possible three-atom sets, scored each set with the same fusion score as in the main method, and measured Recall@1000 for each $\beta \in \{0.0, 0.1, \dots, 1.0\}$. Coherence scores were computed by averaging over all $3!$ atom orderings; availability was scored once per set because the set encoder is permutation-invariant. The matched random baseline is the expected number of held-out sets in a uniformly selected top-1000 set from the same exhaustive candidate space:

$$1000 \cdot \frac{2477}{3,353,896} = 0.739$$

hit sets, or a recall of 2.98×10^{-4} .

Table 11 shows that the ranking is strongly enriched for future papers relative to random. At $\beta = 0$, the top 1000 contains 23 held-out atom sets, corresponding to 28 paper IDs, a $31.1\times$ enrichment over the matched random expectation. The enrichment remains above random through intermediate beta values, but exact recovery declines as unavailability receives more weight. This is expected: $\beta = 0$ asks for the most paper-like triples, while higher β asks for triples that are coherent but less associated with any existing author community. Exact future-paper recovery is therefore not the same objective as alien idea generation.

We also ablate the retrieval cutoff K to check that the prediction signal is not an artifact of choosing top 1000. Figure 19 reports lift over the matched random baseline for $K \in \{100, 1000, 2000, 5000, 10000\}$. The coherence-heavy rankings remain strongly enriched over random across cutoffs: at $\beta = 0$, lift is $13.5\times$ at $K = 100$, $31.1\times$ at $K = 1000$, $31.8\times$ at $K = 2000$, $29.8\times$ at $K = 5000$, and $25.6\times$ at $K = 10000$. The best large-cutoff setting is similar, with $\beta = 0.1$ reaching 191 hits at $K = 10000$, or $25.9\times$ random. By contrast, high- β rankings recover fewer exact 2025 sets at large K , consistent with the interpretation that availability penalization changes the objective away from maximal future-paper recall and toward lower-availability directions.

β	Hit atom sets	Paper IDs	Recall@1000	Lift over random
0.0	23	28	0.0093	31.1×
0.1	11	12	0.0044	14.9×
0.2	10	11	0.0040	13.5×
0.3	7	7	0.0028	9.5×
0.4	7	7	0.0028	9.5×
0.5	5	5	0.0020	6.8×
0.6	2	2	0.0008	2.7×
0.7	3	3	0.0012	4.1×
0.8	3	3	0.0012	4.1×
0.9	0	0	0.0000	0.0×
1.0	0	0	0.0000	0.0×

Table 11: Exact 2025 three-atom set recovery in the exhaustive prediction diagnostic. The random expectation at $K = 1000$ is 0.739 hit atom sets. The strongest exact-recovery setting is pure coherence, but several intermediate beta values remain substantially enriched over random.

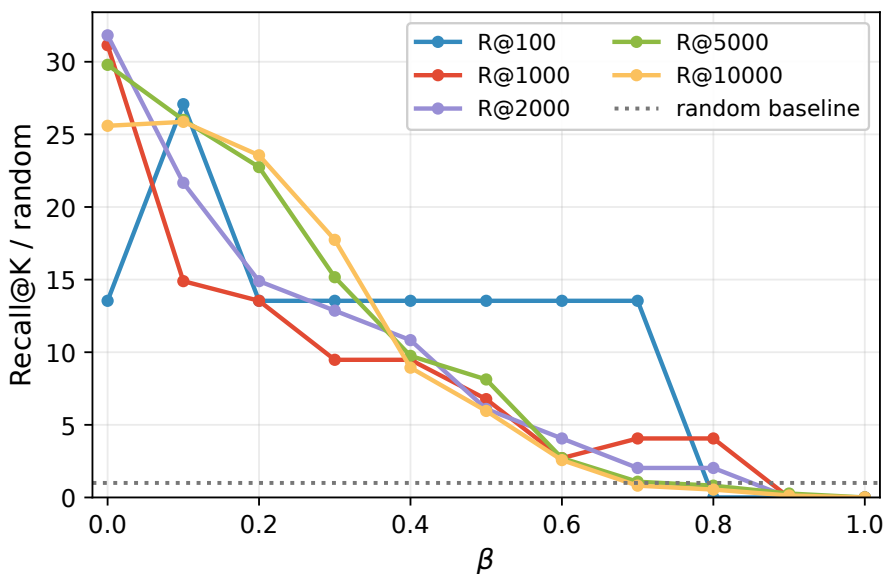


Figure 19: Recall@K sensitivity for the 2025 prediction diagnostic. Each curve shows exact three-atom set recovery normalized by the matched random expectation for the same retrieval cutoff K and candidate space. Coherence-heavy rankings remain strongly enriched over random from $K = 100$ through $K = 10000$, showing that the temporal prediction result is not specific to a single cutoff.

The qualitative composition of the hits changes with β . At $\beta = 0$, the recovered papers mostly belong to dense, central 2025 research areas: code-generation evaluation and environments (*LiveCodeBench* [16], *ConvCodeWorld* [13], and natural-language planning for code generation), efficient inference and compression (*SlimLLM* [15], *SmallKV* [55], online multi-LLM routing, and contrastive routing), multimodal and vision-language modeling (*OmniEdit* [47], *ScImage* [51], *ZoomEye* [35], and statistical factuality for large vision-language models), or alignment or preference learning (*InfAlign* [6], *Language Models Can Predict Their Own Behavior* [4]). This is the behavior expected from a coherence-only score: it identifies future papers in high-density regions of the field, combinations that are known to work.

As β increases, the number of exact hits decreases, but the surviving hits shift toward more selective or bridging directions. Around $\beta = 0.3$ – 0.5 , the recovered papers include *Language Models are Advanced Anonymizers* [40], *LLM-Independent Adaptive RAG* [27], *CARFT: Boosting LLM Reasoning via Contrastive Learning with Annotated Chain-of-Thought-based Reinforced Fine-Tuning* [56], and *Attacking Vision-Language Computer Agents via Pop-ups* [52]. At $\beta = 0.7$ – 0.8 , only three exact-hit papers remain: *Cosmos: Compressed and Smooth Latent Space for Text Diffusion*

Modeling [29], *FocusLLM: Precise Understanding of Long Context by Dynamic Condensing* [24], and *An Efficient and Precise Training Data Construction Framework for Process-supervised Reward Model in Mathematical Reasoning* [42]. These high-beta hits are few, but they are credible future papers at major venues rather than random artifacts. The strongest example is *Cosmos*: at the selected $\beta = 0.7$ setting it appears at rank 19, inside the top 100 triples out of all 3,353,896 candidates, while a random top-100 would contain only 0.074 held-out 2025 triples in expectation. *Cosmos* was accepted as a NeurIPS 2025 poster, with the meta-review emphasizing “solid technical contributions to an underexplored area” as a primary reason for acceptance. This is precisely the kind of case the availability term is intended to surface: not a random or incoherent combination, but a technically viable direction in a less crowded part of the research landscape.

Direct ranking of NeurIPS 2025 papers. We ran a second temporal diagnostic that scores real NeurIPS 2025 papers directly with the same through-2024 coherence and availability models. Instead of enumerating all possible triples, this experiment takes each NeurIPS 2025 paper’s atom set, scores its coherence and unavailability, standardizes scores over the 1,712 scorable NeurIPS 2025 papers, and ranks papers by the same fusion score $(1 - \beta)z_{\text{coh}} + \beta z_{\text{avail}}$ for $\beta \in \{0, 0.025, \dots, 1\}$. This asks a slightly different question: among actual future NeurIPS papers, which ones would the cutoff models have identified as both coherent and low-availability?

In the high-beta neighborhood used by the sampler, the same pattern appears. *Cosmos* is ranked first throughout $\beta = 0.7$ – 0.8 . *Crucible: Quantifying the Potential of Control Algorithms through LLM Agents* rises to rank 2 by $\beta = 0.775$ and remains rank 2 at $\beta = 0.8$; *Meta CLIP 2: A Worldwide Scaling Recipe* reaches rank 3 at $\beta = 0.8$. Thus, at $\beta = 0.8$, the top three ranked NeurIPS 2025 papers are *Cosmos*, *Crucible*, and *Meta CLIP 2*. *Crucible* is a particularly interpretable mixed-direction hit: it combines LLM agents with control-algorithm analysis, using LLM-driven expert simulation to tune control algorithms and quantify their “tuning potential” across control tasks, computer systems, and a real deployment [17]. *Meta CLIP 2*, a NeurIPS 2025 spotlight paper, extends CLIP scaling to worldwide multilingual web data and is also selected by the high-beta ranking [9].

Rank	Paper	Atoms	Coh. rank	Avail. rank
1	<i>Cosmos: Compressed and Smooth Latent Space for Text Diffusion Modeling</i>	3	3	139
2	<i>Crucible: Quantifying the Potential of Control Algorithms through LLM Agents</i>	4	214	140
3	<i>Meta CLIP 2: A Worldwide Scaling Recipe</i>	4	477	66

Table 12: Top NeurIPS 2025 papers under direct paper ranking at $\beta = 0.8$, using coherence and availability models trained only through 2024. Coherence and availability ranks are among the 1,712 scorable NeurIPS 2025 papers, with lower rank indicating stronger coherence or lower modeled availability respectively.

B Conceptual Units and Clustering Validation

We validate the representation layer in two parts. First, we verify that conceptual units preserve the methodology of the original distilled blog post. Second, we choose a clustering method, clustering hyperparameters, and reassignment coverage by testing whether candidate clusters form separable semantic groups.

Conceptual-unit reconstruction. For each paper, we reconstructed the distilled blog post from its paper-specific conceptual units and compared the reconstruction against the original distilled blog. The LLM judge used a five-point scale: full match (5), mostly match (4), partial match (3), minimal match (2), and no match (1), with instructions to evaluate mechanism equivalence rather than exact wording.

Conceptual units received full-match judgments for 97% of evaluated papers. We interpret this as a validation of the extraction step: conceptual units retain enough paper-specific detail to reconstruct the methodological content of the source blog. We do not use this result to claim that clustered atoms can reconstruct papers; atoms are intentionally more abstract and are evaluated separately as a shared vocabulary.

LLM-judge clustering metrics. Clustering quality is semantic: two units should share an atom when they express the same reusable research idea, even if their wording differs. Internal clustering metrics over embeddings do not directly test this property, and the corpus does not provide ground-truth atom labels. We therefore evaluate candidate clusterings with LLM judges over the original unit text.

We use two complementary tests. In the intruder task, the judge receives four units from a source cluster and one unit from a nearby cluster, then identifies the unit that does not belong. Intruder accuracy measures within-cluster purity: if a cluster is coherent, the foreign unit should be easy to detect. In the overlap task, the judge receives four units from each of two nearby clusters and partitions the eight units into two coherent groups. We score the partition with adjusted Rand index (ARI) against the clustering labels. Overlap ARI measures boundary separability: if nearby clusters represent distinct concepts, the judge should recover the same split. We use nearby clusters rather than random pairs so that the tests focus on difficult semantic boundaries. For model selection plots, we summarize both criteria as $Q = (\text{overlap ARI} + \text{intruder accuracy})/2$.

Clustering method and hyperparameter selection. We use the intruder and overlap tests to compare clustering methods and select HDBSCAN hyperparameters. Candidate methods include HDBSCAN on the original embedding space, PCA+HDBSCAN, UMAP+HDBSCAN, and graph clustering variants. For UMAP+HDBSCAN, we sweep UMAP dimensionality and HDBSCAN parameters, including `min_cluster_size`, `min_samples`, cluster selection method, and cluster selection epsilon. Each candidate clustering is evaluated with 200 intruder trials and 200 overlap trials.

Figure 20 summarizes the sweep. Density clustering without dimensionality reduction tends to collapse into very few clusters, which can score well on local purity but is not a useful atom vocabulary. UMAP+HDBSCAN is the strongest non-degenerate family at a useful vocabulary size, and the selected base configuration has $Q = 0.772$ with 250 clusters in the sweep run. Re-running this setting for the final corpus export yields the 273 initial clusters reported above. Figure 21 shows that performance is mostly stable across a broad range of HDBSCAN parameters, with quality improving for moderate-to-large `min_cluster_size` and `min_samples`; this makes the selected setting a conservative operating point rather than a brittle optimum.

The selected configuration uses BGE embeddings, UMAP with 10 dimensions, 30 neighbors, and `min_dist=0.0`, followed by HDBSCAN with `min_cluster_size=15`, `min_samples=15`, `cluster_selection_method=eom`, and `cluster_selection_epsilon=0.0`. This configuration gives high LLM-judged separability before reassignment: intruder accuracy 0.815 and overlap ARI 0.729 in the hyperparameter sweep.

Coverage selection by reassignment. The initial HDBSCAN clustering is conservative: it produces high-purity clusters but leaves 62.8% of units as noise. To choose a usable training representation, we reassign noise units to their nearest cluster centroid in order of embedding similarity and evaluate coverage checkpoints with the same intruder and overlap tests. The purpose is to increase the amount

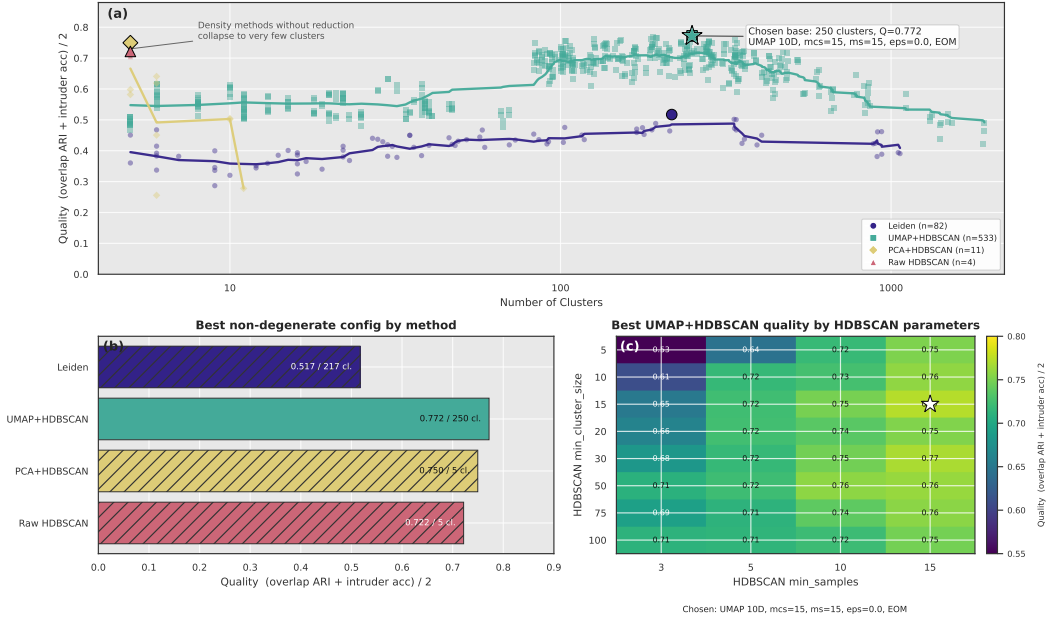


Figure 20: Clustering method and hyperparameter selection. Top: quality as a function of the number of clusters across candidate methods, with the selected UMAP+HDBSCAN base configuration marked. Bottom left: best non-degenerate configuration by method. Bottom right: UMAP+HDBSCAN quality across HDBSCAN min_cluster_size and min_samples. Quality is $Q = (\text{overlap ARI} + \text{intruder accuracy})/2$.

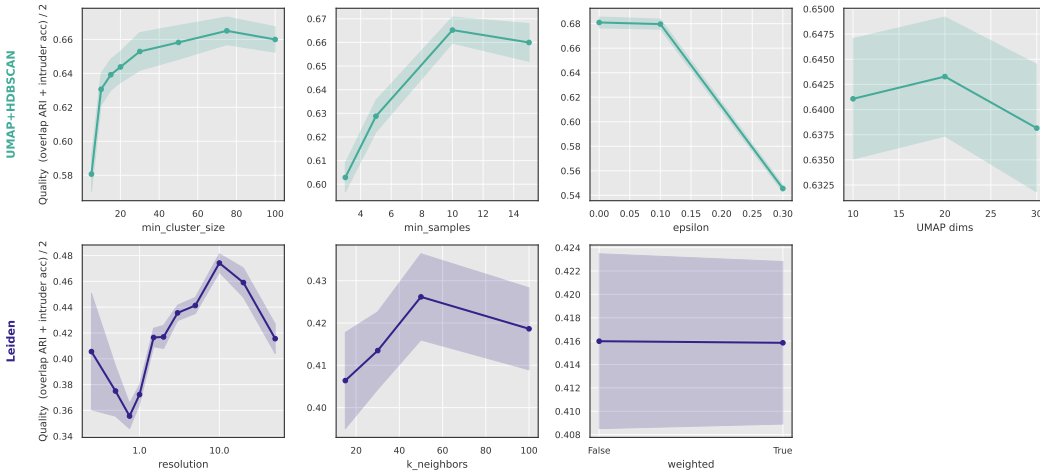


Figure 21: Parameter sensitivity for UMAP+HDBSCAN and Leiden candidates. Lines show mean LLM-judged quality as one parameter varies, with bands indicating variability across the remaining parameters. The selected UMAP+HDBSCAN configuration lies in a broad high-quality region rather than depending on a single narrow parameter setting.

of paper-atom signal available to the models, not to assert that every reassigned unit exactly belongs to its target atom. Reassignment can therefore diffuse some papers into neighboring topics that are close but not identical. The main quantity we want to increase is the average number of atoms per paper: when papers have only one or two atoms, they provide little signal about which atoms co-occur. We select the 80% coverage point because it raises the average from 1.65 to 3.38 atoms per paper, covers 99.5% of papers with at least one atom and 90.6% with at least two, while keeping the minimum reassignment similarity above 0.8. Figure 22 shows this trade-off in the main text.

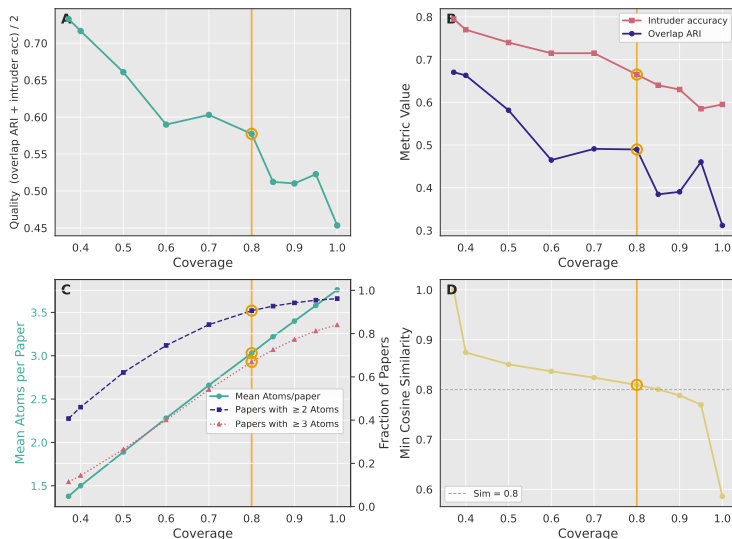


Figure 22: Clustering quality as noise units are reassigned to increase atom coverage. Higher coverage increases the average number of atoms per paper, which is the key source of training signal for the downstream co-occurrence models, but it also makes clusters less semantically pure. We choose 80% coverage: it increases the average from 1.65 to 3.38 atoms per paper while keeping the minimum reassignment similarity above 0.8 and preserving reasonable LLM-judged cluster separability.

With a usable atom representation in hand, we next validate the two scores that define the search objective. Coherence should identify atom sets that plausibly fit into a single paper. Availability should identify atom sets that current author communities are positioned to generate. Before combining them, we test whether each score recovers the intended ordering on controlled pools.

For coherence, we compare exact k -atom paper matches, uniformly random k -sets, and pairwise-disjoint sets whose atom pairs never co-occur in any training paper. Because the coherence model is autoregressive and order-sensitive, each set score marginalizes over all $k!$ permutations and reports $-NLL$, so higher is more coherent. For availability, we compare high-support sets that occur in many author repertoires, uniformly random sets, and zero-support sets absent from every author repertoire. The availability score is the median of the top-10 author-set cosine similarities, so higher means more cognitively available.

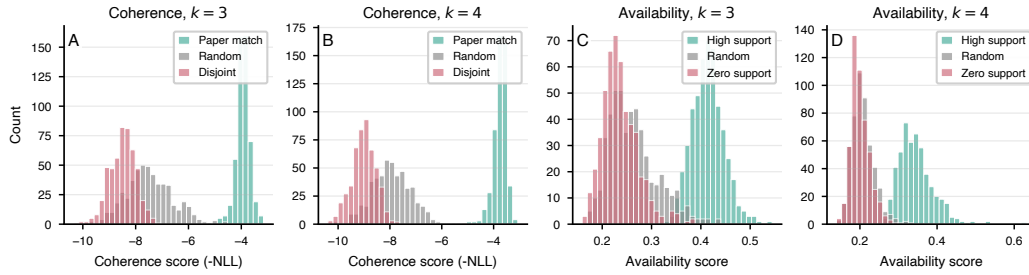


Figure 23: Direct diagnostics of the learned coherence model for $k = 3$ (a) and $k = 4$ (b), and the availability model for $k = 3$ (c) and $k = 4$ (d). Panels (a)–(b) evaluate the coherence model on paper matches, random combinations, and pairwise-disjoint combinations, while panels (c)–(d) evaluate the availability model on combinations with high author support, random support, and zero author support. Higher scores indicate greater coherence in panels (a)–(b) and greater cognitive availability in panels (c)–(d).

Figure 23 shows that both scores behave as intended at $k = 3$ and $k = 4$. The coherence model separates exact paper matches from random combinations and scores disjoint combinations lowest. The availability model assigns high-author-support combinations much higher scores than random or zero-support controls. These diagnostics establish that the two objectives carry distinct usable signal before we combine them for alien sampling.

C Alien Ideas Evaluation

We evaluate the Alien sampler against baselines along three axes: diversity, llm-judge evaluations, and downstream experimental evaluation on an autoresearch agent.

C.1 Experimental Setting

For all generation experiments, we fix the number of atoms per sequence to 3, a compact length near the selected mean of 3.38 atoms per paper.

- **Alien Sampler:** We start with a pool of all possible three-atom sets. We then select the top-300 sequences by the combined coherence–unavailability score.
- **Claude Opus 4.7 and Gemini 3.1 Pro:** Each model is queried 300 times. In each query, the full set of 273 atoms is provided in context, and the model is prompted to select a combination of concepts that is both novel and feasible. The order of atoms is randomly shuffled for every call to mitigate positional bias.
- **Random Baseline:** We randomly sample combinations of atoms 300 times.

For all methods, the selected combinations are reconstructed into natural language research ideas using the same reconstruction pipeline (Section B).

C.2 Diversity Analysis

Using the experimental setting described in Section C.1, we quantify how broadly each method explores the atom vocabulary.

Metrics. We measure diversity using four complementary metrics:

- **Coverage:** Fraction of the total atom vocabulary used across all samples.
- **Gini Coefficient:** Inequality measure where 0 indicates perfect equality (uniform selection) and 1 indicates maximum inequality (all selections from one atom).
- **Mean Repetition:** Average number of times each selected atom is reused across samples.
- **Top-10%:** Fraction of all selections accounted for by the top 10% most frequently selected atoms.

Results. Table C.2 shows diversity metrics across methods.

Method	Unique Atoms	Coverage	Gini	Mean Rep	Top-10%
Random (n=300)	266	97.4%	0.285	3.38	20.3%
Alien sampler ($\beta = 0.7$, n=300)	251	91.9%	0.428	3.59	34.3%
Gemini 3.1 Pro (n=300)	118	43.2%	0.839	7.63	72.6%
Claude Opus 4.7 (n=300)	85	31.1%	0.916	10.59	88.7%

Table 13: Diversity metrics across sampling methods. The Alien sampler achieves diversity comparable to random sampling, while LLMs show severe concentration on a small subset of atoms.

We quantify a critical limitation of LLMs: when prompted to select novel atom combinations, they repeatedly favor the same atoms, limiting diversity. The Alien sampler achieves diversity comparable to random sampling while maintaining coherence.

Analysis of LLM selections reveals systematic biases:

- Both LLM baselines select Sparse Autoencoders as their top atom: Claude includes it in 42.67% of samples and Gemini includes it in 25.67%.
- Claude concentrates heavily on mechanistic-interpretability and reasoning-verification atoms, including concept vectors, activation patching, Process Reward Models, and symbolic verification.
- Gemini is less concentrated than Claude but still repeatedly selects Sparse Autoencoders, Flow Matching, activation steering, machine unlearning, and biophysical-constraint modeling.

- The Alien sampler is substantially flatter: its two most frequent atoms appear in only 5.33% of samples, and its top atoms span neuro-computational alignment, misinformation defense, alignment behavior mapping, AI red-teaming, and lexical ambiguity.

Top Atoms by Method. Below we show the three most frequently selected atoms for each non-random generation method. Percentages in parentheses indicate the fraction of the 300 samples that included the atom. Atom labels are typeset in sans serif to distinguish canonical atom identities from ordinary prose.

Claude Opus 4.7.

1. **Atom 111** (42.67%): *Sparse Autoencoders (SAEs) resolve the problem of neural superposition—where individual neurons simultaneously encode multiple, overlapping concepts—by functioning as dictionary learners that project dense, polysemantic model activations into a higher-dimensional latent space constrained by sparsity. This mechanism decomposes complex internal representations into discrete, ‘monosemantic’ features, where each active dimension corresponds to a single, human-interpretable concept. By isolating these individual computational primitives, SAEs enable researchers to transparently audit a neural network’s internal logic, map causal feature circuits, and perform precise, surgical interventions on specific behaviors without the need for opaque fine-tuning.*
2. **Atom 178** (34.00%): *High-level semantic concepts and behavioral traits in neural networks are encoded as distinct linear directions within high-dimensional activation spaces, a phenomenon formalized as the Linear Representation Hypothesis. These specific ‘concept vectors’ can be mathematically isolated through contrastive activation analysis—calculating the vector difference between the internal states of paired inputs representing opposing traits (e.g., true versus false, or safe versus harmful) to cancel out shared syntactic and contextual noise. Once isolated, these vectors enable direct operational control, allowing researchers to mathematically probe a network’s latent cognitive states or surgically steer its behavior during generation by adding or subtracting the concept vector, entirely bypassing the need for model retraining.*
3. **Atom 183** (24.33%): *Activation patching—along with variants like path patching and interchange intervention—is a causal interpretability technique that isolates the functional components of a neural network by surgically transplanting internal activations from a source execution run into a counterfactual or corrupted target run; if this targeted substitution alters or restores the model’s final prediction to match the source, it definitively identifies the patched layers, tokens, or neural circuits as the causally responsible pathways for that specific reasoning step or behavior.*

Gemini 3.1 Pro.

1. **Atom 111** (25.67%): *Sparse Autoencoders (SAEs) resolve the problem of neural superposition—where individual neurons simultaneously encode multiple, overlapping concepts—by functioning as dictionary learners that project dense, polysemantic model activations into a higher-dimensional latent space constrained by sparsity. This mechanism decomposes complex internal representations into discrete, ‘monosemantic’ features, where each active dimension corresponds to a single, human-interpretable concept. By isolating these individual computational primitives, SAEs enable researchers to transparently audit a neural network’s internal logic, map causal feature circuits, and perform precise, surgical interventions on specific behaviors without the need for opaque fine-tuning.*
2. **Atom 9** (22.33%): *Flow Matching unifies diverse generative and alignment tasks by learning a continuous vector field that defines deterministic, optimal transport trajectories between a source distribution, such as random noise or sub-optimal model states, and a target data distribution. By modeling transformations as Ordinary Differential Equations that move samples along mathematically efficient, straight-line or geodesic paths, this approach bypasses the complex, stochastic iterative denoising of traditional diffusion models and the sequential predictions of autoregressive models, resulting in faster inference, enhanced training stability, and precise control for generating complex multi-dimensional data or steering model behaviors.*
3. **Atom 177** (14.67%): *Inference-time activation steering enables causal control over neural network behavior without weight fine-tuning by isolating high-level concepts—such as truthfulness, safety, or reasoning style—as specific directional vectors within the model’s latent space. By dynamically intervening on a model’s internal hidden states along these conceptual axes during the forward pass, researchers can robustly align outputs to desired traits, bypassing the vulnerabilities of external prompt manipulation while utilizing targeted calibrations to preserve the model’s foundational capabilities and linguistic fluency.*

Alien Sampler.

1. **Atom 17** (5.33%): *Neuro-computational alignment utilizes regularized linear mapping techniques—such as Ridge Regression—to project the high-dimensional internal latent activations of artificial intelligence models onto localized biological neural activity recorded via methods like fMRI or MEG. This mathematical bridging acts as an ‘encoding model’ that allows researchers to quantify the representational and temporal*

similarity between digital architectures and human cognitive processing. By establishing this cross-domain translation, scientists can empirically verify if artificial systems converge on evolutionary computational solutions, map specific computational mechanisms to anatomical brain regions, and use biological neural signals as a direct training target to fine-tune artificial models for greater functional and semantic fidelity.

2. **Atom 68 (5.33%)**: *Advanced misinformation defense transcends static, binary fact-checking by conceptualizing deception as a dynamic, evolutionary process of semantic distortion and persuasive manipulation. Employing interpretable mechanisms—such as multidimensional semantic taxonomies, bottleneck reasoning traces, and adversarial synthetic generation—decouples factual veracity from stylistic presentation to expose underlying rhetorical strategies. Analyzing the continuous mutation of claims enables artificial intelligence systems to generate contextual explanations and proactive inoculations, empowering audiences to recognize and resist sophisticated, evolving false narratives.*
3. **Atom 198 (4.00%)**: *Advancing artificial intelligence alignment beyond binary 'safe/unsafe' classification involves mapping model behaviors and reasoning traces onto multidimensional vector spaces grounded in validated psychometric frameworks (such as Moral Foundations Theory) and formal ethical philosophies (such as Deontology and Utilitarianism). Operationalizing machine ethics through value pluralism transforms abstract morality into measurable computational variables, enabling researchers to quantify an agent's unique 'moral fingerprint,' mathematically evaluate how it dynamically resolves conflicts between competing social goods, and audit the underlying logical rationale of its decisions across diverse cultural contexts.*

C.3 Pairwise LLM Judge Evaluation of Generated Ideas

The diversity and novelty metrics above measure whether a method explores a broad, less familiar region of idea space. They do not directly ask whether the resulting ideas would be preferred as research directions. We therefore ran a complementary forced-choice LLM-judge evaluation over decoded idea descriptions. Each comparison showed two methodology sketches without method labels, and the judge selected the sketch that better satisfied the coherent cognitive-unavailability criterion: plausible enough to investigate, but less likely to arise from current ML labs, prevailing toolchains, or frontier LLM ideation patterns. The prompt explicitly treated risk as acceptable when attached to a coherent high-upside bet, and asked whether the idea opens a new framing, research object, empirical target, or line of follow-on work rather than merely specifying a convenient first experiment.

We used GPT-5.5 with medium reasoning effort, temperature 1.0, and JSON-mode forced-choice outputs. The tournament design was deliberately simple. In the full round, we used 50 ideas per method. For each unordered method pair and each of three seeds, we sampled 20 one-to-one cross-method comparisons, avoiding duplicate unordered idea pairs where possible and balancing A/B presentation sides. With four methods this gives $6 \times 3 \times 20 = 360$ pairwise judgments, all usable. We then ran two elimination diagnostics: select the top half of each method by item-level wins in the previous round and repeat the same balanced design with 25 ideas per method and 10 comparisons per method pair per seed (180 judgments), then select the top 10 per method and repeat with 4 comparisons per method pair per seed (72 judgments). These elimination rounds are a tail-concentration diagnostic, not an independent absolute-quality benchmark: selection and evaluation intentionally share the same coherent-unavailability criterion. We exclude a later 5-idea diagnostic from the main plot because the pool is too small for stable method-level conclusions.

Method	Full 50	Top 25	Top 10
Random	41.1%	41.1%	41.7%
Alien sampler ($\beta = 0.7$)	55.6%	72.2%	69.4%
Gemini 3.1 Pro	54.4%	58.9%	58.3%
Claude Opus 4.7	48.9%	27.8%	30.6%

Table 14: Raw method win rates in the coherent-unavailability pairwise judge. Each entry is the fraction of all matches involving that method that the method won in the corresponding round.

Method	Full 50	Top 25	Top 10
Random	0.763	0.749	0.766
Alien sampler ($\beta = 0.7$)	1.184	2.109	1.888
Gemini 3.1 Pro	1.144	1.336	1.305
Claude Opus 4.7	0.967	0.474	0.530

Table 15: Bradley–Terry method abilities fit separately within each judge round and normalized so that the method mean is 1. Scores above 1 indicate above-average pairwise preference under the coherent-unavailability judge for that round.

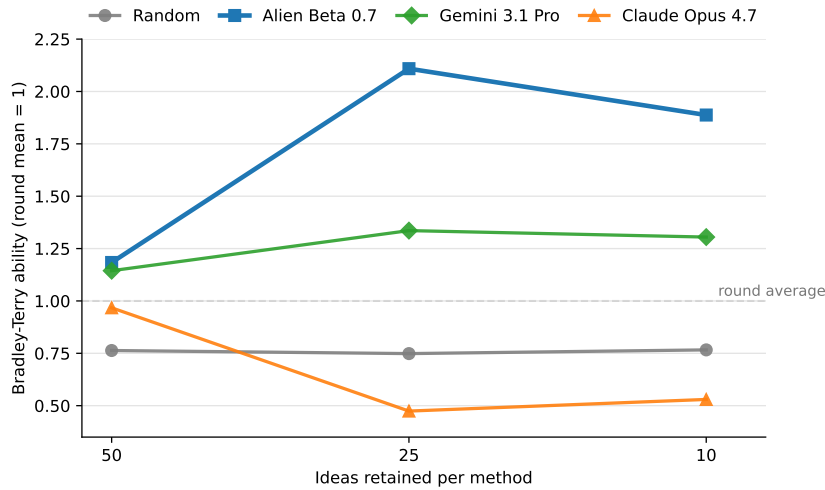


Figure 24: Bradley–Terry method abilities across elimination rounds. Alien strengthens sharply after selecting the top half of each method’s outputs, while the random baseline remains flat and Claude drops under the coherent-unavailability criterion.

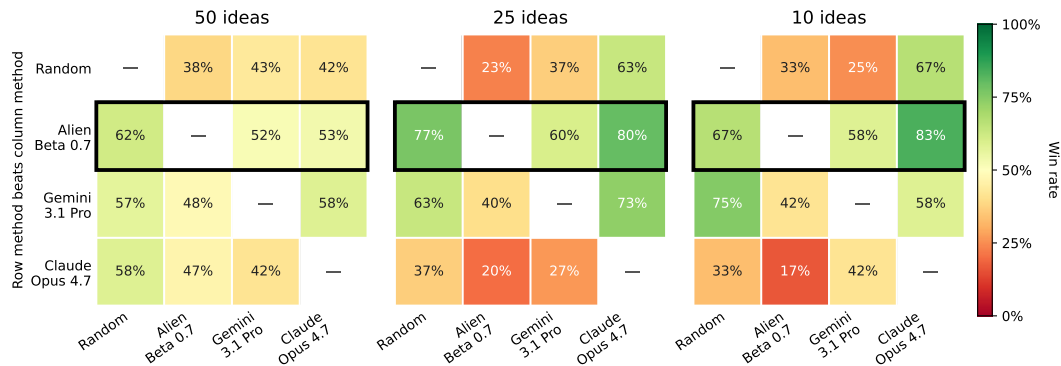


Figure 25: Pairwise win-rate matrices for the same judge rounds. Each cell is the row method’s win rate against the column method; the diagonal is omitted. The black outline highlights the Alien sampler row.

D Downstream Evaluation Details

We ran two downstream evaluations beyond atom-level diversity, novelty, and coherence. First, human raters evaluated the generated idea descriptions directly. Second, we ran a fixed autoresearch pipeline that turned each generated idea into a bounded empirical research note, then evaluated the resulting notes with blind pairwise LLM judgments. These evaluations are small, but they test a different question from the atom metrics: whether generated ideas remain useful once interpreted as concrete research directions.

D.1 Human Survey

We collected 40 clean human reviews, 10 per source method. Reviewers rated each idea on coherence, feasibility, novelty, promise, obviousness, and overall quality using five-point scales. Table 16 reports pooled means and standard errors. The results are close: Alien and Claude tie on overall quality, Alien has the highest feasibility and novelty means, and Claude has the highest promise and core-score means.

Method	n	Coherence	Feasibility	Novelty	Promise	Overall
Alien	10	4.20 ± 0.20	3.90 ± 0.23	3.90 ± 0.28	4.10 ± 0.18	4.03 ± 0.11
Claude	10	4.30 ± 0.30	3.60 ± 0.22	3.80 ± 0.29	4.40 ± 0.27	4.03 ± 0.23
Gemini	10	4.00 ± 0.33	3.20 ± 0.29	3.70 ± 0.37	3.80 ± 0.39	3.68 ± 0.30
Random	10	3.70 ± 0.21	3.70 ± 0.21	3.60 ± 0.22	4.00 ± 0.15	3.75 ± 0.04

Table 16: Human ratings of generated idea descriptions. Entries are means \pm standard errors over clean reviews.

Survey instrument. The survey was self-administered through a private web app via per-rater unique URLs; no identifying information was collected beyond a study-issued panelist ID. After a short instructions screen (Figure 26), each rater saw four idea blogposts one at a time (Figure 27); the source method of each idea was hidden. A read gate (Figure 28) disabled the rating button for the first 45 seconds of each idea to enforce a minimum reading window. The rating form (Figure 29) then collected a brief free-text summary, five ordinal ratings on five-point scales (coherence, feasibility, obviousness, novelty, and worthwhileness), and a short free-text justification.

D.2 Autoresearch Pipeline and Pairwise Report Judging

For each source method, we selected 10 generated ideas and ran the same autoresearch pipeline. The pipeline used Claude Code CLI v2.1.101 with the `claude-sonnet-4-6` model setting on Mila compute nodes with optional A100 40GB GPU access. Each run consisted of a deep-research stage, an experimenter stage, a writer stage, a critic stage, and one experimenter–writer repair loop. The final artifact was a standalone `research_note.md`.

The 40 reports were anonymized and evaluated with blind pairwise preference judgments. We used a six-round Swiss-style comparison schedule: reports were paired against nearby reports in the current ordering, duplicate unordered pairings were avoided where possible, and each scheduled comparison was shown in both A/B and B/A order. Pairwise preferences were converted into rankings using Bradley–Terry scores, and method quality was summarized by average rank percentile over the full 40-idea pool, where rank 1 maps to 1.0 and rank 40 maps to 0.0.

Method	Avg. rank percentile	Reports	Top 5	Top 10	Median rank
Alien	0.633	10	3	4	14.5
Claude	0.574	10	1	4	14.0
Gemini	0.495	10	1	2	24.0
Random	0.295	10	0	0	28.0

Table 17: LLM-judge rankings of autoresearch reports. Average rank percentile is computed over the full 40-idea pool.

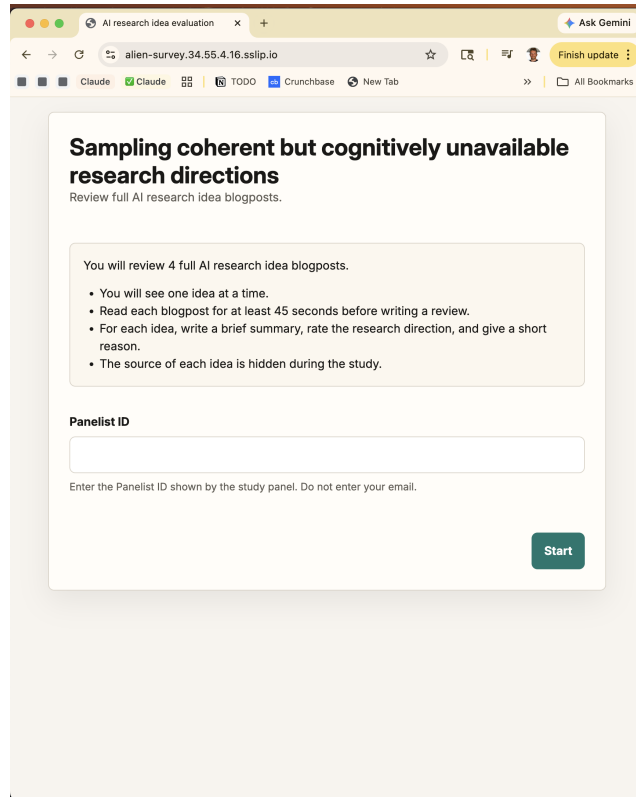


Figure 26: Human survey landing page. Reviewers entered a study-issued panelist ID and read brief instructions before starting. Each session covered four idea blogposts, presented one at a time, with the source method of each idea hidden.

D.3 Motif Concentration in Autoresearch Reports

We coded each original idea title and each final report for membership in a sparse-autoencoder / feature-level mechanistic-interpretability cluster. A report counts once if it uses SAE or sparse-feature language, or feature-level interpretability machinery such as activation steering, causal tracing, activation patching, concept vectors, monosemantic features, or polysemantic representations. Generic uses of words such as “mechanistic” or “interpretable” were not counted.

Method	Original titles in cluster	Final reports in cluster
Alien	0/10	0/10
Claude	2/10	8/10
Gemini	4/10	5/10
Random	0/10	1/10

Table 18: Concentration around the SAE / feature-level mechanistic-interpretability cluster before and after autoresearch. Claude and Gemini reports are much more likely to route through this toolkit than Alien reports.

D.4 Idea Identity Preservation

As a sanity check, we asked whether the autoresearch pipeline preserves the identity of the starting idea. For each completed final report, we embedded the final report and all 40 original idea titles with `text-embedding-3-small`. We then ranked all original titles by cosine distance to the final report and recorded the rank of the report’s own starting title. If the pipeline preserves idea identity, the final report should be nearest, or at least very close, to its own original title.

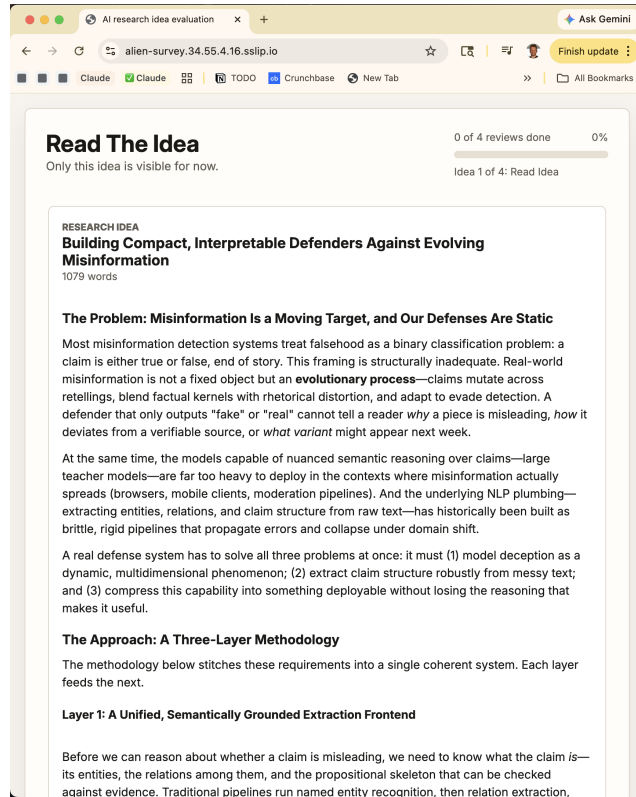


Figure 27: Idea reading view. Each blogpost was rendered in full (with the title and word count shown above the body) and only the current idea was visible at any time. A progress indicator on the top right tracked completion across the four ideas.

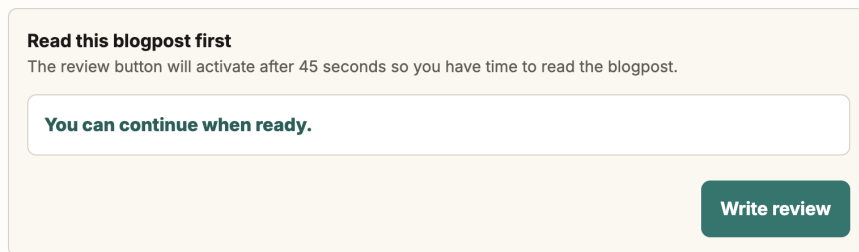


Figure 28: Read gate. The “Write review” button was disabled for the first 45 seconds on each idea, enforcing a minimum reading window before any rating could be entered.

The identity-preservation result suggests that the autoresearch pipeline is not simply rewriting all ideas into unrelated generic reports. However, final reports are still more stylistically and semantically similar to each other than the initial titles, as expected from a shared empirical-report format and bounded experimentation pipeline. We therefore treat title-to-report nearest-neighbor preservation as a sanity check, and treat motif concentration as the more interpretable downstream diversity diagnostic.

E Example Outputs

E.1 Example Atoms

Below we show example atoms along with representative constituent conceptual units. The **Atom** field contains the canonical description passed to the LLM during reconstruction, the general idea

Write a brief summary of the idea

How coherent is this as a research direction?

1 2 3 4 5

Not coherent Very coherent

How likely is this idea to work?

1 2 3 4 5

Very unlikely Very likely

How likely is it that a typical active AI/ML researcher would independently propose this idea?

1 2 3 4 5

Very unlikely Very likely

How novel is this idea?

1 2 3 4 5

Not novel Very novel

How worthwhile would this be for a researcher or lab to pursue?

1 2 3 4 5

Not worthwhile Very worthwhile

Brief reason for your ratings

Next idea

Figure 29: Rating form. For each idea, reviewers wrote a brief free-text summary, rated five ordinal dimensions on five-point scales—coherence (“How coherent is this as a research direction?”), feasibility (“How likely is this idea to work?”), obviousness (“How likely is it that a typical active AI/ML researcher would independently propose this idea?”), novelty (“How novel is this idea?”), and worthwhileness (“How worthwhile would this be for a researcher or lab to pursue?”)—and provided a short free-text justification.

Method	Final reports	Own title nearest	Own title in top 3	Mean own-title rank
Alien	10	7	8	2.40
Claude	10	7	9	2.30
Gemini	10	8	9	2.60
Random	8	3	6	2.88

Table 19: Title-level identity preservation through the autoresearch pipeline. Most final reports remain closest, or close, to their own starting idea title.

captured by the atom. The **LLM justification** explains what the clustered units have in common, the analysis the LLM does on the conceptual units before naming the atom.

Atom Example: Sparse Autoencoders

Atom 111: Sparse Autoencoders (SAEs) resolve the problem of neural superposition—where individual neurons simultaneously encode multiple, overlapping concepts—by functioning as dictionary learners that project dense, polysemantic model activations into a higher-dimensional latent space constrained by sparsity. This mechanism decomposes complex internal representations into discrete, ‘monosemantic’ features, where each active dimension corresponds to a single, human-interpretable concept. By isolating these individual computational primitives, SAEs enable researchers to transparently audit a neural network’s internal logic, map causal feature circuits, and perform precise, surgical interventions on specific behaviors without the need for opaque fine-tuning.

LLM justification: *The cluster uniformly focuses on the application of Sparse Autoencoders (SAEs) and dictionary learning in mechanistic interpretability. The common thread is the mechanism of projecting dense, overlapping neural activations into a higher-dimensional, sparse space to resolve 'polysemanticity' (superposition). This effectively decomposes messy signals into distinct, single-concept ('monosemantic') features, enabling researchers to transparently audit internal logic, map causal circuits, and surgically steer model behavior.*

Constituent Conceptual Units:

1. Sparse Autoencoders (SAEs) can disentangle conceptual 'superposition' in neural networks—where single neurons represent multiple unrelated concepts—by projecting hidden activations into a higher-dimensional space where individual features map to specific, interpretable semantic concepts.
2. Sparse Autoencoders (SAEs) can act as 'interpretable dictionaries' for opaque models by mapping dense, entangled internal representations into a high-dimensional, sparse latent space where each active dimension corresponds to a single, monosemantic concept.
3. Training objectives for Sparse Autoencoders balance a reconstruction error (ensuring the sparse code preserves the original data's information) with an L1 regularization penalty that forces the model to represent complex inputs using the smallest possible set of active concepts.
4. Sparse Autoencoders can interpret opaque neural network activations by projecting them into a high-dimensional, sparse hidden layer; this decomposes complex internal signals into a set of nearly independent 'feature directions' that correspond to human-understandable concepts like 'baseball' or 'ships'.
5. Feature discovery in neural networks can be categorized into three primary approaches: unsupervised methods (like Sparse Autoencoders) that find hidden structures without labels, supervised subspace methods (like Distributed Alignment Search) that learn rotations of neural space to find causal directions for specific labels, and masking methods (like Differential Binary Masking) that identify discrete subsets of existing neurons responsible for a concept.
6. Sparse Autoencoders (SAEs) facilitate model interpretability and control by decomposing dense, polysemantic neural activations into a high-dimensional space of sparse, individual features, allowing researchers to 'clamp' specific features to influence model output.
7. Sparse Autoencoders (SAEs) address the problem of neural superposition—where a single activation represents multiple, entangled concepts—by decomposing dense hidden states into thousands of sparse, monosemantic features that each correspond to a single, human-understandable concept.
8. Mechanistic interpretability tools like Sparse Autoencoders offer an alternative to prompt engineering by identifying specific neural features that correlate with task performance, enabling researchers to directly amplify these internal representations to steer the model toward desired outputs more precisely.
9. Sparse Autoencoders (SAEs) can be used to decompose the polysemantic, high-dimensional activation space of Large Language Models into a set of sparse, interpretable linear directions called 'latents,' which isolate specific conceptual features that would otherwise be overlapping and messy.
10. Neural superposition occurs in Large Language Models when single neurons represent multiple unrelated concepts simultaneously to increase efficiency; Sparse Autoencoders (SAEs) can mitigate this by mapping messy activations into a high-dimensional space where individual 'features' represent specific, human-understandable concepts.
11. ... (88 additional conceptual units omitted)

Atom Example: Code Structure Graphs

Atom 253: Transforming source code from linear text into explicit structural and semantic representations—such as Abstract Syntax Trees, control-flow graphs, and project-wide dependency networks—decouples underlying algorithmic logic from surface-level syntax. This architectural abstraction enables language models and automated systems to transcend token-based context

limitations by navigating software as an interconnected topology, allowing them to systematically resolve non-local dependencies, extract minimal viable execution contexts, enforce deterministic semantic rules, and perform complex reasoning tasks across large-scale, multi-file repositories.

LLM justification: *The cluster revolves around the limitation of treating source code as flat text and the necessity of using formal graph-based abstractions (ASTs, Control Flow Graphs, Dependency Trees, etc.) to capture programming logic. By mapping codebase architecture, these structural tools constrain and guide language models, allowing them to manage context windows, resolve distant dependencies, and reason accurately about project-wide semantics.*

Constituent Conceptual Units:

1. Structural filtering using Abstract Syntax Tree (AST) analysis—which maps code into a hierarchical representation of its logical operations—allows training systems to identify functional equivalence between snippets, ensuring that code with identical execution logic is treated as similar even if its surface-level text or naming differs.
2. Professional software development is characterized by high interdependency, where research indicates that roughly 73% of functions in large-scale repositories rely on project-specific modules, internal utilities, or local architectural patterns rather than being self-contained.
3. A distinction exists between 'static' code features (properties visible without execution, like token count) and 'dynamic' code features (properties that emerge during runtime, like the number of execution steps), which are processed by different cognitive subsystems during mental simulation.
4. Complex software repositories can be converted into portable, executable units by tracing the dependency tree of a specific target file—analyzing imports and internal file paths—to extract only the essential code and data needed for that specific functionality, creating a 'compact workspace.'
5. Software library evolution can be modeled as a Knowledge Graph where API elements are nodes and version transitions (such as renames or parameter updates) are directed edges; this enables the calculation of a cumulative 'net change' between non-adjacent versions by traversing and merging the transformation rules across multiple version jumps.
6. Variable definitions located in remote directories can be recovered for code completion context by traversing a repository-level dataflow graph from the point of use, following logical dependencies back to their source assignments and type declarations regardless of file structure.
7. Source code foundation models can be utilized as parametric knowledge bases where, instead of retrieving existing code from an external database, the model is 'probed' to synthesize new code fragments that explain the logic of low-level machine instructions.
8. A 'Removal-then-Completion' strategy for code generation addresses potential errors in a user's draft by stripping away partial implementations and generating code based solely on high-level specifications (like docstrings) to ensure a clean, functional foundation.
9. Performance bottlenecks in complex software can be identified by applying PageRank-style ranking to program call graphs, where execution costs are propagated from callees to callers to rank functions based on their cumulative influence on overall system performance.
10. Software 'domain' can be categorized into a hierarchy of granularity—including organization, project/repository, and module/folder—meaning that a distributional shift in code models can occur at various levels of stylistic and architectural context.
11. ... (90 additional conceptual units omitted)

E.2 Example Research Ideas

Below we show example research ideas generated by the Alien Sampler and by Claude Opus 4.7. Each example shows the input atoms and the reconstructed natural language research idea produced by the reconstruction pipeline.

Atoms:

- Formal grammar frameworks—such as Context-Free Grammars and their probabilistic extensions—serve as deterministic bridges between abstract mathematical logic and complex natural language. By enforcing explicit, hierarchical rules for syntax generation and parsing, these frameworks allow researchers to exert rigorous control over structural complexity. This structural determinism is utilized to generate unbiased, procedurally complex synthetic datasets, strictly constrain neural agent outputs to valid logical action spaces, and establish absolute mathematical ground truths. Consequently, researchers can isolate and evaluate a machine learning model’s underlying syntactic reasoning, spatial logic, and predictive uncertainty entirely independently from real-world semantic confounders or benchmark memorization.
- To overcome the ‘plausibility trap’—where artificial intelligence explanations sound convincing but fail to represent the system’s actual logic—the structural faithfulness of a model’s interpretability is quantified through causal perturbation and predictive reconstruction frameworks. By employing mechanisms such as necessity and sufficiency testing (ablating or isolating key features to observe proportional shifts in model confidence) alongside simulatability tasks (where independent proxy models attempt to reproduce the original decision using solely the generated explanation), researchers can objectively verify that an interpretable narrative maps directly to the true parametric mechanisms and causal pathways driving the system’s output.
- Iterative self-improvement loops enable machine learning models to autonomously bootstrap their capabilities by functioning as both data generators and evaluators. By producing synthetic outputs, filtering them through automated verification mechanisms—such as self-consistency checks, environmental execution, or adversarial self-critique—and fine-tuning on the resulting high-quality reasoning trajectories or isolated error cases, models establish a recursive training flywheel. This continuous feedback cycle progressively shifts the learning frontier, allowing models to transcend the limitations of their initial training distributions, master increasingly complex tasks, and significantly reduce reliance on human-annotated labels.

Research Idea:

Grammar-Grounded Self-Improvement with Faithful Interpretability

The Problem: Reasoning Models We Can Neither Trust Nor Verify

Modern machine learning models, especially those trained on web-scale corpora, suffer from three interlocking failure modes that prevent them from being reliable reasoners.

First, **evaluation is contaminated**. When we test reasoning on natural-language benchmarks, we cannot disentangle genuine inference from memorization, semantic shortcut-taking, or distributional priors baked in during pretraining.

Second, **explanations lie**. A model can produce a fluent chain-of-thought rationale that bears no causal relationship to the parameters that actually produced its answer. This “plausibility trap” makes interpretability tools dangerous when used as trust signals: they sound right, but verify nothing.

Third, **improvement is bottlenecked by human labels**. Scaling reasoning capability by hand-annotating ever-harder problems is expensive, slow, and ultimately capped by what annotators themselves can solve.

This methodology proposes a unified research approach that addresses all three problems simultaneously by combining **formal grammars as a structural backbone**, **causal interpretability tests for faithfulness**, and **self-improvement loops for capability expansion**.

The Approach: A Three-Layer Methodology

The core idea is to build the entire training and evaluation pipeline on top of a **formal grammar substrate**, then use that substrate to (a) guarantee ground truth, (b) verify the faithfulness of model explanations, and (c) drive iterative self-improvement on synthetic but rigorously specified tasks.

Layer 1: Formal Grammars as the Ground-Truth Substrate

We start by adopting context-free grammars (and their probabilistic extensions) as the generative engine for the task universe. A grammar is a deterministic bridge between abstract mathematical logic and natural-language-like structure: it specifies, hierarchically and explicitly, what counts as a well-formed input and what counts as a valid derivation.

This choice is consequential:

- **Procedurally generated, unbiased datasets.** Because we control the grammar, we can sample arbitrarily complex examples without accidentally embedding the regularities of any particular human corpus. The complexity dial—nesting depth, production-rule branching factor, ambiguity—is ours to turn.
- **Hard ground truth.** For every generated sample, the grammar yields the correct parse, the correct logical structure, and the correct answer. There is no annotator disagreement.
- **Constrained action spaces.** When a neural agent emits outputs (e.g., a derivation, a parse, or a decision sequence), we can require those outputs to lie inside the grammar. Invalid productions are simply unrepresentable. This eliminates a large class of trivial errors and isolates genuine reasoning failures.
- **Confounder-free evaluation.** Because the inputs are synthetic and procedurally diverse, benchmark memorization is impossible. What remains, when a model succeeds, is an estimate of its actual syntactic and structural reasoning ability.

In short: the grammar gives us a sandbox where every claim about the model’s reasoning can, in principle, be checked against an absolute reference.

Layer 2: Faithfulness via Causal Perturbation and Simulatability

Having ground truth is necessary but not sufficient. A model that produces correct answers may still be producing wrong *explanations*—reasoning traces that look principled but don’t reflect the mechanism that actually generated the prediction.

To break the plausibility trap, we evaluate explanations using two complementary causal tests:

1. **Necessity and sufficiency testing.** For each feature, intermediate step, or rule application that an explanation cites as load-bearing, we perform targeted ablations and isolations. If the explanation says “step k of the derivation determined the answer,” then ablating step k should produce a proportional drop in the model’s confidence, and providing only step k should approximately recover the prediction. Disproportionate or absent shifts are evidence that the explanation is not causally faithful.
2. **Simulatability.** We hand the generated explanation—and only the explanation—to an independent proxy model and ask it to reproduce the original system’s decision. An explanation that genuinely captures the decision pathway should make the original output predictable from itself; one that is decorative will not.

Crucially, both tests are *quantitative*. Faithfulness becomes a measurable property rather than a vibe. And because the underlying tasks come from the grammar substrate, we know the true causal structure that explanations *should* be tracking, giving these faithfulness scores a meaningful upper bound.

Layer 3: Self-Improvement Driven by Verifiable Synthetic Signal

The third layer turns the system into a recursive training flywheel. The model plays both roles in its own curriculum:

- **As a generator**, it produces candidate solutions, derivations, or reasoning trajectories on grammar-sampled problems.
- **As an evaluator**, it filters those candidates using automated verification: self-consistency across multiple samples, execution against the grammar (does this parse? does this derivation reach the target?), or adversarial self-critique where one pass tries to falsify another.

Verified-correct trajectories become high-quality fine-tuning data. Persistent failure modes become hard-example sets for targeted training. Because verification is grounded in the grammar—not in another fallible model’s opinion—the filtering signal is trustworthy.

Iterating this loop has a striking effect: the model’s competence frontier shifts outward. Each round of fine-tuning enables it to solve slightly harder grammar-sampled problems, which in turn become the seed material for the next round. Reliance on human-labeled supervision drops

sharply, and the model can move into regions of task complexity that no annotator was ever asked to cover.

Why the Three Layers Need Each Other

Each layer fails on its own; together, they form a closed loop.

- **Grammars without self-improvement** give us a clean evaluation but no path to scaling capability.
- **Self-improvement without grammars** is dangerous: without absolute verification, the model's filter is itself biased, and the flywheel can amplify its own errors.
- **Self-improvement without faithfulness checks** produces models that get better at the task but increasingly opaque, and we cannot distinguish genuine reasoning gains from sophisticated pattern matching.
- **Faithfulness checks without grammars** lack a reliable referent: we can show that an explanation is internally causal, but not that it tracks the *correct* causal structure.

When stitched together, the methodology works as follows. The grammar defines the problem space and supplies ground truth. The model bootstraps its capabilities through verified self-generated data, filtered against grammar-grounded checks. At each stage, its explanations are stress-tested via necessity/sufficiency ablation and simulatability, ensuring that capability gains are accompanied by genuinely faithful internal reasoning—not merely better-sounding rationalizations.

Takeaway for Practitioners

If you are building reasoning systems and want to escape the trio of memorization, plausible-but-empty explanations, and label scarcity, the recipe is: anchor your task distribution in a formal grammar; constrain model outputs to that grammar; use causal perturbation and simulatability to audit explanations; and close the loop with self-generated, grammar-verified training data. The grammar is what makes everything else honest.

Alien Sampler – Example Idea 2

Atoms:

- Continuous relaxation transforms discrete sequence generation into a differentiable optimization problem by representing discrete variables—such as text tokens—as continuous probability distributions, soft logits, or dense embeddings. By applying gradient descent to these continuous proxies and systematically projecting the updated vectors back into discrete space using techniques like straight-through estimators, Voronoi partitioning, or gradient-guided coordinate substitution, the intractability of combinatorial discrete search is bypassed. This paradigm allows complex constraints, sequential dependencies, and targeted objective functions to be efficiently optimized across entire high-dimensional language sequences simultaneously.
- Continuous relaxations and gradient estimation techniques—such as the Gumbel-Softmax trick, Straight-Through Estimators, and Hard Concrete distributions—enable end-to-end gradient-based optimization of neural networks containing discrete, non-differentiable operations. By mathematically transforming hard categorical selections, binary pruning masks, and architectural routing decisions into smooth probability distributions or surrogate gradients, continuous approximations allow standard backpropagation algorithms to simultaneously optimize continuous model parameters and discrete structural or sequential choices.
- Translating artificial personas from superficial stylistic mimicry into stable psychological simulations requires decomposing human identity into multi-dimensional constructs that combine standardized psychometric traits, episodic memory anchors, and distinct cognitive styles. By enforcing these structured profiles through explicit behavioral constraints, in-character self-reflection loops, and specialized architectural routing, AI agents resist collapsing into a generic baseline, enabling both the quantifiable validation of virtual identities via clinical psychological inventories and the deployment of behaviorally consistent synthetic populations for complex social modeling.

Research Idea:

Optimizing Discrete Personas: A Gradient-Based Approach to Stable Psychological Simulation in Language Models

The Problem: Personas That Collapse

When we ask large language models to roleplay as specific individuals — a clinically anxious teenager, a stoic engineer, a citizen with particular political leanings — they tend to drift. After a few turns, surface mimicry erodes and the model regresses toward a generic, helpful baseline. This is not merely an aesthetic flaw. It is a fundamental obstacle for any application that needs *behaviorally consistent synthetic populations*: social simulation, clinical training, agent-based modeling, or stress-testing policies on virtual cohorts.

The root cause is that "being a persona" is not a single objective. It is a **discrete, structured commitment**: a choice of psychometric trait levels, a particular set of episodic memories, a cognitive style that shapes how the agent reasons. Each of these decisions is categorical or combinatorial, and current LLMs handle them only through prompting — a brittle, non-optimized channel.

This blog sketches a methodology that treats persona instantiation as a **differentiable optimization problem over discrete identity structure**, fusing three threads: continuous relaxation of discrete generation, gradient-based optimization of discrete architectural choices, and a multi-dimensional psychological decomposition of identity itself.

The Core Idea

Rather than hand-engineer prompts or fine-tune on imitation data, we represent every discrete component of a persona — token choices in self-narrations, on/off memory activations, and routing decisions to specialized cognitive modules — as a continuous proxy that can be optimized end-to-end. We then project these continuous proxies back into discrete persona behavior, and we validate the resulting agents against established clinical psychometric inventories.

The methodology has three layers, each addressing one super-atom.

Layer 1: Continuous Relaxation of Persona Utterances

A persona is ultimately observable through what it says. To optimize what it says against a target psychological profile, we need gradients through token selection. We use the standard toolkit:

- **Soft logits and dense embedding proxies** stand in for hard token IDs during the forward pass.
- **Gradient descent on these continuous representations** allows us to push outputs toward objectives like trait-consistency, memory-faithfulness, or style adherence.
- **Projection back to discrete tokens** uses straight-through estimators, Voronoi partitioning over the embedding space, or gradient-guided coordinate substitution to anchor the soft optimum to a real token sequence.

This converts the intractable combinatorial search over "what would *this* person say next?" into smooth optimization across an entire response simultaneously. Sequential dependencies and global constraints (e.g., "the response must reflect high neuroticism *and* reference the character's childhood event") become joint objectives rather than greedy decoding heuristics.

Layer 2: Gradient-Based Optimization of Discrete Architecture

A stable persona is more than its utterances; it has internal *structure*. Some memories should be active in some contexts, others suppressed. Different cognitive styles should route through different sub-networks: an analytical persona might engage a chain-of-thought module, an impulsive one might bypass it.

These are inherently discrete decisions — binary memory masks, categorical routing — and they too need to be learned, not hardcoded. Here we apply the second super-atom:

- **Gumbel-Softmax** for categorical routing among cognitive-style modules.
- **Hard Concrete distributions** for binary masks gating which episodic memories are accessible.
- **Straight-Through Estimators** for any remaining hard selections.

Crucially, this lets standard backpropagation jointly optimize *continuous* model parameters (the language model weights or adapter parameters) and *discrete* structural choices (which

memories, which modules, which traits dominate). The persona is not just a prompt — it is an architectural configuration that is itself learned.

Layer 3: A Structured Psychological Profile as the Optimization Target

Layers 1 and 2 are useless without a well-posed target. The third super-atom supplies it: a persona must be decomposed into multi-dimensional constructs:

1. **Standardized psychometric traits** (e.g., Big Five-style continuous trait vectors) provide the quantitative skeleton.
2. **Episodic memory anchors** — concrete biographical events — provide the narrative substrate that prevents traits from being abstract numbers.
3. **Distinct cognitive styles** define *how* the persona reasons, not just *what* it believes.

These three dimensions are then enforced through:

- **Explicit behavioral constraints** that enter the loss function (e.g., trait-prediction heads scoring generated text).
- **In-character self-reflection loops**, in which the model critiques its own output through the persona’s lens, providing additional gradient signal.
- **Specialized architectural routing** (the discrete choices from Layer 2) that physically separates cognitive modes.

Because the target is structured and quantitative, we can validate — not just vibe-check — the resulting agents by administering **clinical psychological inventories** and comparing scores to the target profile.

Putting It Together

The training/inference loop looks like this:

1. **Specify** a target persona as (trait vector, memory set, cognitive-style assignment).
2. **Generate** candidate behavior using soft logits / embedding proxies (Layer 1).
3. **Score** the soft generation against the structured psychological target — trait classifiers, memory-grounding checks, style adherence — and against in-character self-reflection critiques (Layer 3).
4. **Backpropagate** through the soft generation and through Gumbel-Softmax / Hard Concrete gates that control memory access and module routing (Layer 2).
5. **Project** soft outputs back to discrete tokens, and harden routing/memory masks at deployment.
6. **Validate** the deployed agent by administering psychometric inventories; iterate if scores deviate from the target.

Why It Works

Each layer plugs a hole the others cannot:

- **Without Layer 1**, we cannot get gradient signal into the actual utterances; we are stuck doing prompt engineering.
- **Without Layer 2**, the persona has no internal structure that resists collapse; memories and reasoning modes degenerate into a soft average.
- **Without Layer 3**, optimization has no principled target — we mimic surface style rather than simulating identity.

Together, they convert persona construction from a prompting craft into a well-defined optimization problem with measurable outcomes. The same continuous-relaxation machinery that has been used to optimize adversarial text or prune networks is repurposed to sculpt stable psychological agents — and the same psychometric instruments used on humans become the validation harness for synthetic ones.

The payoff is populations of LLM agents that don’t drift, whose differences are quantifiable, and whose internal structure is the product of learning rather than improvisation.

Atoms:

- The 'cross-modal alignment gap' in Vision-Language Models exposes a critical safety vulnerability where models heavily aligned to refuse harmful discrete text fail to generalize those guardrails to continuous visual embeddings. Attackers exploit this geometric mismatch by distributing malicious intent across modalities, embedding harmful text visually, or pairing individually benign images and prompts to create emergent harm; therefore, securing these systems requires enforcing safety boundaries directly on fused internal activations, ensuring that the integrated multi-modal context reliably maps to the model's latent refusal mechanisms.
- High-level semantic concepts and behavioral traits in neural networks are encoded as distinct linear directions within high-dimensional activation spaces, a phenomenon formalized as the Linear Representation Hypothesis. These specific 'concept vectors' can be mathematically isolated through contrastive activation analysis—calculating the vector difference between the internal states of paired inputs representing opposing traits (e.g., true versus false, or safe versus harmful) to cancel out shared syntactic and contextual noise. Once isolated, these vectors enable direct operational control, allowing researchers to mathematically probe a network's latent cognitive states or surgically steer its behavior during generation by adding or subtracting the concept vector, entirely bypassing the need for model retraining.
- Sparse Autoencoders (SAEs) resolve the problem of neural superposition—where individual neurons simultaneously encode multiple, overlapping concepts—by functioning as dictionary learners that project dense, polysemantic model activations into a higher-dimensional latent space constrained by sparsity. This mechanism decomposes complex internal representations into discrete, 'monosemantic' features, where each active dimension corresponds to a single, human-interpretable concept. By isolating these individual computational primitives, SAEs enable researchers to transparently audit a neural network's internal logic, map causal feature circuits, and perform precise, surgical interventions on specific behaviors without the need for opaque fine-tuning.

Research Idea:**Closing the Cross-Modal Safety Gap with Sparse, Interpretable Concept Steering****The Problem: Safety Doesn't Survive the Jump to Vision**

Vision-Language Models (VLMs) inherit the safety alignment of their text backbones, but that alignment turns out to be surprisingly brittle once a vision encoder is bolted on. The root cause is what we might call the **cross-modal alignment gap**: refusal behaviors are heavily trained against *discrete* harmful text tokens, but the visual pathway feeds the model *continuous* embeddings that occupy a different region of the representation space. The guardrails simply don't generalize geometrically.

Attackers have learned to weaponize this mismatch. They render harmful instructions as images (bypassing text-side filters entirely), or distribute malicious intent *across* modalities — pairing an innocuous image with an innocuous prompt that, only when fused, produces emergent harm. Because the harmful signal lives in the *combined* internal state rather than in either input alone, input-level moderation is structurally insufficient.

The conclusion is uncomfortable but clear: safety must be enforced on the **fused internal activations** themselves, where the integrated multi-modal context actually meets the model's latent refusal machinery. The question is how to do that surgically — without retraining the model, and without breaking benign behavior.

The Approach: Read the Latent State, Then Steer It

The methodology we describe combines two complementary mechanistic-interpretability tools to inspect and intervene on a VLM's fused activations:

1. **Contrastive activation analysis** to identify directions in activation space that correspond to safety-relevant concepts (e.g., "harmful intent" vs. "benign request").
2. **Sparse autoencoders (SAEs)** to decompose dense, polysemantic activations into discrete, monosemantic features, so the steering directions we recover are interpretable and precisely targeted rather than entangled with unrelated behaviors.

Together these give us a way to (a) *probe* whether a fused multi-modal context has crossed an internal safety boundary, and (b) *steer* the model back toward refusal when it has — all without fine-tuning.

Step 1: Isolate concept vectors via contrastive activation

The Linear Representation Hypothesis tells us that high-level semantic traits — truthfulness, sentiment, harmfulness, refusal — tend to be encoded as **linear directions** in a model’s activation space. We can recover such a direction by collecting paired inputs that differ only along the trait of interest (a harmful request vs. its benign counterpart, both delivered through the same modality configuration), running each through the VLM, and taking the **vector difference** of their fused internal states at a chosen layer.

The contrastive subtraction is doing real work: shared syntactic structure, formatting tokens, and context-specific noise cancel out, leaving a vector that points along the axis the model itself uses to distinguish the two conditions. Crucially, because we collect these activations *after* fusion of vision and language tokens, the resulting concept vector lives in the same space where cross-modal attacks actually manifest.

Once isolated, a concept vector is operational. We can:

- **Probe** by projecting an unseen fused activation onto it, asking “how harmful does this combined context look from the inside?”
- **Steer** by adding or subtracting the vector during generation to push the model toward or away from refusal — entirely bypassing retraining.

Step 2: Disentangle with sparse autoencoders

Raw concept vectors derived from contrastive pairs work, but they ride on top of a representation in **superposition**: individual neurons (and the activation directions they span) encode many overlapping concepts at once. A “harmfulness” direction recovered naively can entangle with topic, tone, or modality artifacts, producing brittle interventions that misfire on benign inputs. This is exactly the problem SAEs are designed to solve. An SAE trained on the model’s fused-layer activations acts as a **dictionary learner**, projecting dense activations into a much higher-dimensional, sparsely-active latent space. The sparsity constraint forces each active dimension to specialize, yielding **monosemantic features** that correspond to single, human-interpretable concepts.

In our setting, this means we can:

- Decompose the fused activation of a harmful multi-modal input into its constituent SAE features.
- Identify the small set of features that consistently activate on harmful content across modalities — including cases where harm is conveyed visually or only emerges from the image-text combination.
- Use those features (rather than raw activation directions) as the substrate for steering, giving us interventions that are precise and auditable.

Step 3: Enforce safety on fused activations

Putting the pieces together, the runtime defense looks like this:

1. The VLM processes a multi-modal input and produces fused internal activations at a target layer.
2. The SAE decomposes those activations into monosemantic features; the relevant safety-related features are inspected.
3. A contrastively-derived refusal direction — sharpened by the SAE decomposition — is used either as a **detector** (flagging inputs whose fused state crosses the harmfulness boundary) or as a **steering vector** (added to activations to restore refusal behavior in real time).

Because all of this happens on the *fused* internal state, it is invariant to which modality smuggled in the harmful content. Visually-rendered text, benign-looking image+prompt pairs that only become harmful when combined, and ordinary text jailbreaks all converge to the same internal signature, where the intervention can act.

Why It Works

Three properties make this synthesis robust:

- **It targets the right surface.** Cross-modal attacks succeed because input-level safety checks see each modality in isolation. Operating on fused activations meets the attack where it actually lives.
- **It is mechanistic, not behavioral.** Rather than patching outputs after the fact, we identify the model’s own internal representation of harm and act on it directly. The Linear Representation Hypothesis gives us a principled reason to expect such a direction to exist; contrastive analysis gives us a way to find it.
- **It is surgical.** SAEs cut through superposition so that interventions affect the intended concept and little else. This is what makes activation steering practical as a safety mechanism rather than a blunt instrument: we can audit *which* feature we’re modulating and verify it corresponds to the behavior we care about.

The broader point is that the cross-modal safety gap is not solved by training harder on the input side. It is solved by recognizing that safety is ultimately a property of the model’s internal state, and by using interpretability tools — linear concept vectors and sparse, monosemantic features — to make that internal state legible and controllable.

Claude Opus 4.7 – Example Idea 2

Atoms:

- Sparse Autoencoders (SAEs) resolve the problem of neural superposition—where individual neurons simultaneously encode multiple, overlapping concepts—by functioning as dictionary learners that project dense, polysemantic model activations into a higher-dimensional latent space constrained by sparsity. This mechanism decomposes complex internal representations into discrete, ‘monosemantic’ features, where each active dimension corresponds to a single, human-interpretable concept. By isolating these individual computational primitives, SAEs enable researchers to transparently audit a neural network’s internal logic, map causal feature circuits, and perform precise, surgical interventions on specific behaviors without the need for opaque fine-tuning.
- Activation patching—along with variants like path patching and interchange intervention—is a causal interpretability technique that isolates the functional components of a neural network by surgically transplanting internal activations from a source execution run into a counterfactual or corrupted target run; if this targeted substitution alters or restores the model’s final prediction to match the source, it definitively identifies the patched layers, tokens, or neural circuits as the causally responsible pathways for that specific reasoning step or behavior.
- Process Reward Models enhance complex artificial intelligence reasoning by shifting evaluation from final-outcome validation to granular, step-by-step verification. By assigning localized success probabilities to individual intermediate actions within a logical chain, these models solve the credit assignment problem and eliminate outcome bias caused by flawed logic that coincidentally yields a correct answer. This continuous, step-level supervision acts as a computational critic that enables advanced search algorithms to dynamically prune erroneous branches, trigger targeted self-correction, and optimally scale inference-time compute to isolate the most robust logical trajectory.

Research Idea:

Opening the Black Box of Reasoning: A Mechanistic Approach to Auditing Step-Level Logic

The Problem: We Can Score Reasoning, But We Can’t See It

Modern language models perform impressive multi-step reasoning, but our tools for understanding *how* that reasoning works remain crude. We typically evaluate a chain of thought by checking whether the final answer is correct—a coarse signal that conflates lucky guesses with sound logic and gives us no insight into where reasoning actually happens inside the network. Worse, when a model produces a flawed intermediate step, outcome-based supervision can reinforce the bad logic so long as the answer happens to land right.

This creates two intertwined gaps:

1. **A behavioral gap.** We lack reliable, step-level signals for which intermediate moves in a reasoning chain are actually correct.
2. **A mechanistic gap.** Even when we know a step is wrong, we don't know which internal components of the model produced it, nor what concepts those components were representing.

A methodology that closes both gaps would let us not only catch faulty reasoning, but *localize it inside the model* and *intervene on it* without retraining.

The Approach: Step-Level Verification Coupled to Mechanistic Localization

The methodology synthesizes three complementary tools, each addressing one stage of an end-to-end auditing pipeline for reasoning:

- **Process Reward Models (PRMs)** to detect *where* in a reasoning chain something goes wrong.
- **Sparse Autoencoders (SAEs)** to expose *what concepts* the model is representing at that moment.
- **Activation patching** to verify *which components* are causally responsible for the step.

Used together, these form a loop: localize-in-trajectory → decompose-in-representation → confirm-with-causation.

Step 1: Use a Process Reward Model to Localize Failure in the Reasoning Trajectory

A PRM scores each intermediate step in a chain rather than only the final answer. By assigning a localized success probability to every action, it solves the credit-assignment problem and removes the outcome bias that plagues end-to-end evaluation. In our pipeline, the PRM plays two roles:

- **As a search critic at inference time**, it lets us prune branches that derail, trigger self-correction, and concentrate compute on the most robust logical trajectories.
- **As a diagnostic flag**, it pinpoints the specific token positions and steps where the model's reasoning probability collapses—giving us a precise *site of interest* to investigate mechanistically.

The PRM, in other words, converts the vague question "what went wrong?" into "what happened at step k of the chain?" That handoff is what makes the rest of the pipeline tractable.

Step 2: Decompose the Activations at the Failure Site with Sparse Autoencoders

At the flagged step, the model's hidden state is dense and polysemantic: individual neurons simultaneously encode many overlapping concepts due to superposition. Reading these activations directly tells us little.

We project them through a Sparse Autoencoder trained to act as a dictionary learner—mapping dense activations into a much higher-dimensional, sparsity-constrained latent space. In that space, only a handful of features fire, and each active feature ideally corresponds to a single, human-interpretable concept (a "monosemantic" feature).

This decomposition turns the failure site into something readable. Instead of staring at a vector of opaque numbers, we see a short list of concepts the model was attending to when its reasoning faltered—candidate hypotheses for *what the model was actually doing*.

Step 3: Confirm Causality with Activation Patching

Interpreted features are still only correlational. To establish that a specific concept, layer, or attention pathway *causally* drove the faulty step, we use activation patching and its variants (path patching, interchange interventions).

The protocol:

1. Run the model on the original (failing) chain and a counterfactual chain that should produce the correct step.
2. Surgically transplant activations—from particular layers, tokens, or even SAE feature directions—from one run into the other.
3. Observe whether the model's prediction at that step flips accordingly.

If patching the candidate component restores or breaks the behavior, we have causal evidence that this component carries the reasoning step. Combined with the SAE decomposition, this lets us say not just "circuit *X* is responsible" but "circuit *X*, encoding concept *C*, is responsible."

Why the Three Components Fit Together

Each technique compensates for the weakness of the others:

- **PRMs without mechanistic tools** tell us a step is wrong but not why; they operate purely at the behavioral surface.
- **SAEs without PRMs** produce mountains of features with no principled way to know which ones to look at; the PRM provides the targeting signal.
- **SAEs without patching** yield interpretive hypotheses that may be epiphenomenal; patching disciplines interpretation with causal tests.
- **Patching without SAEs** can identify a responsible layer or head but leaves the *content* of its computation unreadable, since superposed activations resist semantic labeling.

The result is a pipeline whose outputs are far richer than any component alone:

- **Trajectory:** Question answered: At which step did reasoning fail? Tool: Process Reward Model.
- **Representation:** Question answered: What concepts were active at that step? Tool: Sparse Autoencoder.
- **Causation:** Question answered: Which components actually drove the step? Tool: Activation patching.

Implications: From Auditing to Surgical Intervention

Once a faulty reasoning step has been localized in the trajectory, decomposed into interpretable features, and causally pinned to specific components, intervention becomes targeted rather than blunt. Rather than fine-tuning the entire model and hoping the bad behavior is overwritten, a practitioner can suppress or amplify specific SAE features, or block specific patched pathways, at exactly the steps the PRM flags.

This methodology reframes interpretability from a post-hoc curiosity into an operational loop: *detect bad reasoning step-by-step, explain it in human concepts, prove the explanation causally, and act on it surgically*. It treats the reasoning chain as the natural unit of analysis—long enough to contain real logic, short enough that mechanistic tools can reach inside each link.